OUTP-0930P
CERN-PH-TH-259

Testing SUSY at the LHC: Electroweak and Dark matter fine tuning at two-loop order.

S. Cassel [a], **D. M. Ghilencea** [b,*], **G. G. Ross** [a,b,†]

[a] Rudolf Peierls Centre for Theoretical Physics, University of Oxford, 1 Keble Road, Oxford OX1 3NP, United Kingdom.

[b] Department of Physics, CERN - Theory Division, CH-1211 Geneva 23, Switzerland.

Abstract

In the framework of the Constrained Minimal Supersymmetric Standard Model (CMSSM) we evaluate the electroweak fine tuning measure that provides a quantitative test of supersymmetry as a solution to the hierarchy problem. Taking account of current experimental constraints we compute the fine tuning at two-loop order and determine the limits on the CMSSM parameter space and the measurements at the LHC most relevant in covering it. Without imposing the LEPII bound on the Higgs mass, it is shown that the fine tuning computed at two-loop has a minimum $\Delta = 8.8$ corresponding to a Higgs mass $m_h = 114 \pm 2$ GeV. Adding the constraint that the SUSY dark matter relic density should be within present bounds we find $\Delta = 15$ corresponding to $m_h = 114.7 \pm 2$ GeV and this rises to $\Delta = 17.8$ ($m_h = 115.9 \pm 2$ GeV) for SUSY dark matter abundance within 3σ of the WMAP constraint. We extend the analysis to include the contribution of dark matter fine tuning. In this case the overall fine tuning and Higgs mass are only marginally larger for the case SUSY dark matter is subdominant and rises to $\Delta = 28.7$ ($m_h = 116.98 \pm 2$ GeV) for the case of SUSY dark matter saturates the WMAP bound. For a Higgs mass above these values, fine tuning rises exponentially fast. The CMSSM spectrum that corresponds to minimal fine tuning is computed and provides a benchmark for future searches. It is characterised by heavy squarks and sleptons and light neutralinos, charginos and gluinos.

*on leave from Theoretical Physics Department, IFIN-HH Bucharest MG-6, Romania.
†e-mail addresses: s.cassel1@physics.ox.ac.uk, dumitru.ghilencea@cern.ch, g.ross1@physics.ox.ac.uk

Contents

1 Introduction

With the Large Hadron Collider up and running, the search for TeV-scale SUSY is now significantly closer. Many models of physics beyond the Standard Model (SM), in particular its minimal supersymmetric version (MSSM), will be directly tested. To do so, one has to quantify the viable range of parameters entering in these models, which impact in particular on the scale of its low-energy supersymmetric spectrum. Previous theoretical and experimental constraints such as those from LEP have already tested a considerable amount of the MSSM parameter space and identified bounds on it. To study these bounds further it is instructive to investigate from a quantitative perspective the impact of the, so far, negative searches for

low-energy supersymmetry. A quantitative measure of this impact is the fine-tuning measure Δ [1, 2], that quantifies the degree of cancellation between unrelated parameters that is needed to fix the electroweak scale and can be extended to include the fine tuning needed to obtain an acceptable dark matter abundance. In this paper we shall perform such an investigation, computing Δ at two-loop leading log order in the Constrained MSSM (CMSSM). For previous studies of the fine-tuning problem in a similar context see [1]-[18].

The electroweak fine-tuning measure, Δ, provides a measure of the probability of unnatural cancellations of soft masses in the expression of the electroweak scale $v^2 \sim -\sum_i m^2_{soft,i}/\lambda$, ($\lambda$ is Higgs quartic coupling) after including quantum corrections. So Δ measures the stability of the MSSM electroweak scale at the quantum level, with all available experimental and theoretical constraints imposed. These include the LEP mass bounds on supersymmetry masses, charge/colour breaking constraints, the dark matter relic density constraint, and the measurement of $b \to s\gamma$ and the anomalous magnetic moment of the muon. In what follows we identify the constraints with the largest impact on Δ. We also extend the analysis to include the fine tuning, Δ^Ω, needed to satisfy the constraints on the SUSY dark matter abundance. The method can be readily extended to other models that claim to solve the hierarchy problem. For the case that the fine tuning is reduced by new states with mass well above the TeV range, one may extend the analysis using the effective Lagrangian in which the very heavy states have been integrated out. For fine tuning and related issues in such scenarios see for example [17, 20, 21, 22, 23], where the MSSM Higgs mass can be increased nearer the LEP bounds by classical effects due to new physics beyond few TeV, which ultimately reduces the fine tuning.

The fine-tuning problem in the MSSM is important not only for supersymmetry searches, but also for the Higgs physics since it is intrinsically related to the value of the lightest Higgs mass m_h, currently restricted by the LEPII lower bound of 114.4 GeV [19]. As a result searches for m_h are relevant to supersymmetry phenomenology. In particular, the need to increase the SUSY prediction for the Higgs mass by radiative corrections above the LEPII bound means that the electroweak fine tuning measure rises exponentially with the Higgs mass. If Δ becomes too large one can conclude that SUSY fails to provide a solution to the hierarchy problem. The parameter configuration (consistent with the non-observation of SUSY states) that minimises Δ gives an indication of its most likely values. We identify this configuration and investigate its phenomenological implications. Also for a given upper value of Δ one can extract the corresponding range of parameter space of the CMSSM and of the

superpartners masses.

In Section 2 we present the calculation of the electroweak fine tuning measure to two loop order. We are not aware of a similar analysis of the fine tuning problem at this level of precision (two-loop leading log), which is responsible for a Δ smaller than that usually found in the literature. In Section 3 we discuss the dependence of the fine tuning on $\tan\beta$ and the impact on the fine tuning coming from imposing the bounds on the SUSY spectrum and the limits on $b \to s\gamma$. Using the dependence of the fine tuning measure on the parameters of the CMSSM we then determine their allowed range consistent with a given value of Δ. This provides a quantitative measure of the remaining parameter space range that remains to be tested. Next we determine the dark matter abundance as a function of the fine tuning measure showing that low fine tuning is consistent with acceptable SUSY dark matter abundence. We conclude this Section by considering the implications for the Higgs mass following from requiring low fine tuning. We show that, without imposing the LEPII bound on the Higgs mass, Δ has a minimum for a region of m_h near the LEPII bound. In Section 4 we extend the fine tuning analysis to include the fine tuning needed either to satisfy the dark matter bound or to saturate the bound with SUSY dark matter. Finally in Section 5 we discuss the predictions for the superpartner mass spectrum from the fine tuning bound. We also determine the most likely spectrum that minimises fine tuning and discuss the relative importance of various LHC measurements in the test of the CMSSM. Section 6 presents a summary and our conclusions.

2 Computing electroweak scale fine-tuning Δ at two-loop level

In this section we present the strategy for evaluating the MSSM fine-tuning at tree, one-loop and two-loop (leading log) level; particular attention is paid to clarifying the impact on fine tuning of the quantum corrections to couplings and masses. With the standard two-Higgs doublet notation, the scalar potential is

$$\begin{aligned} V &= m_1^2\,|H_1|^2 + m_2^2\,|H_2|^2 - (m_3^2\; H_1\cdot H_2 + h.c.) \\ &+ \frac{1}{2}\,\lambda_1\,|H_1|^4 + \frac{1}{2}\,\lambda_2\,|H_2|^4 + \lambda_3\,|H_1|^2\,|H_2|^2 + \lambda_4\,|H_1\cdot H_2|^2 \\ &+ \left[\frac{1}{2}\,\lambda_5\;(H_1\cdot H_2)^2 + \lambda_6\;|H_1|^2\,(H_1\cdot H_2) + \lambda_7\;|H_2|^2\,(H_1\cdot H_2) + h.c.\right] \end{aligned} \tag{1}$$

The couplings λ_j and the soft masses receive one- and two-loop corrections that for the MSSM

are found in [24, 25]. We shall use these results to evaluate the overall amount of fine-tuning of the electroweak scale. Technical details of the procedure can be found in the Appendix.

To evaluate the fine-tuning, it is convenient to introduce the notation

$$\begin{aligned} m^2 &= m_1^2 \cos^2\beta + m_2^2 \sin^2\beta - m_3^2 \sin 2\beta \\ \lambda &= \frac{\lambda_1}{2}\cos^4\beta + \frac{\lambda_2}{2}\sin^4\beta + \frac{\lambda_{345}}{4}\sin^2 2\beta + \sin 2\beta\left(\lambda_6\cos^2\beta + \lambda_7 \sin^2\beta\right) \end{aligned} \tag{2}$$

with the assumption that, in the MSSM, at the UV scale $m_1^2 = m_2^2 = m_0^2 + \mu_0^2$ while $m_3^2 = B_0\,\mu_0$. The couplings λ_j are assumed to be real and $\lambda_{345} = \lambda_3 + \lambda_4 + \lambda_5$. In[1] the MSSM, at the tree level they are

$$\lambda_1 = \lambda_2 = 1/4\,(g_1^2 + g_2^2), \quad \lambda_3 = 1/4\,(g_2^2 - g_1^2), \quad \lambda_4 = -1/2\,g_2^2, \quad \lambda_{5,6,7} = 0 \tag{3}$$

where $g_{1,2}$ are the $U(1)$ and $SU(2)$ gauge couplings respectively.

The fine-tuning amount wrt to a set of parameters $\{p\}$ of the MSSM is then [1, 2]

$$\Delta \equiv \max\left|\Delta_p\right|_{p=\{\mu_0^2, m_0^2, m_{1/2}^2, A_0^2, B_0^2\}}, \qquad \Delta_p \equiv \frac{\partial \ln v^2}{\partial \ln p} \tag{4}$$

where all p are input parameters at the UV scale of CMSSM, in the standard notation[2] The minimisation of V gives

$$v^2 = -m^2/\lambda, \qquad 2\lambda\frac{\partial m^2}{\partial\beta} = m^2\frac{\partial\lambda}{\partial\beta} \tag{5}$$

which fix v and β as functions of the above MSSM bare parameters. Taking into account that $m^2 = m^2(p,\beta)$, $\lambda = \lambda(p,\beta)$ we can find $\partial\beta/\partial p$ from the second minimum condition for V. Using this, one finds[3] [11], see also [17]:

$$\begin{aligned} \Delta_p &= -\frac{p}{z}\left[\left(2\frac{\partial^2 m^2}{\partial\beta^2} + v^2\frac{\partial^2\lambda}{\partial\beta^2}\right)\left(\frac{\partial\lambda}{\partial p} + \frac{1}{v^2}\frac{\partial m^2}{\partial p}\right) + \frac{\partial m^2}{\partial\beta}\frac{\partial^2\lambda}{\partial\beta\partial p} - \frac{\partial\lambda}{\partial\beta}\frac{\partial^2 m^2}{\partial\beta\partial p}\right] \\ z &= \lambda\left(2\frac{\partial^2 m^2}{\partial\beta^2} + v^2\frac{\partial^2\lambda}{\partial\beta^2}\right) - \frac{v^2}{2}\left(\frac{\partial\lambda}{\partial\beta}\right)^2 \end{aligned} \tag{6}$$

[1] When using the Yukawa couplings at the low energy scale as an input, expressed in terms of the Higgs vev and quark masses, then m and λ pick up additional, implicit dependence on $v = \langle h\rangle$ and $\tan\beta$. Neglecting this dependence when evaluating Δ_p does not bring significant changes to the results for final Δ.

[2] One could also include in the set of parameters p, the top Yukawa coupling or the strong coupling α_3. For such parameters which are measured, one can use the modified fine tuning definition [26] and with this, it turns out that in the cases we consider their associated fine tuning never dominates.

[3] Later the min condition (fixing β) is used to replace B_0 by $\tan\beta$ as an independent parameter.

This result takes into account the dependence of β on the MSSM set of parameters (p). This formula also takes into account the loop-effects to the quartic couplings as well as the $\tan\beta$ dependence of the radiative corrections on the parameter "p". As we shall see later, such effects tend to reduce fine-tuning, in many cases rather significantly[4].

For comparison with similar studies of fine-tuning, a comment is in place here. After some algebra, one can show that the general formula of Δ (eqs.(4), (6)) reduces, in the limit of removing the loop corrections to quartic couplings λ_i, $i = 1, 2...$, to the more familiar "master formula" [28] (see also [4, 5])

$$\Delta_p = \frac{p}{(\tan^2\beta - 1)\, m_Z^2}\left\{\frac{\partial m_1^2}{\partial p} - \tan^2\beta\,\frac{\partial m_2}{\partial p} - \frac{\tan\beta}{\cos 2\beta}\left[1 + \frac{m_Z^2}{m_1^2 + \tilde{m}_2^2}\right]\left[2\frac{\partial m_3^2}{\partial p} - \sin 2\beta\left(\frac{\partial m_1^2}{\partial p} + \frac{\partial m_2^2}{\partial p}\right)\right]\right\} \qquad (7)$$

This formula is sometimes used as the starting point in works that evaluate electroweak scale fine-tuning, by using in it the loop corrected soft masses. However, for accurate estimates, it is necessary to take full account of radiative corrections, as done by eqs.(4), (6). Indeed, the loop corrections to the quartic couplings significantly reduce the amount of fine-tuning, in some cases by a factor as large as 2, and these corrections are not accounted for by eq.(7). This can be seen by considering the one-loop correction δ to $\lambda_2 \to \lambda_2(1+\delta)$, due to stop/top Yukawa couplings. Usually $\delta = \mathcal{O}(1)$. Including it one finds (for details see eq.(26) in [17]):

$$\Delta_p \propto \frac{p}{(1+\delta)\, m_Z^2} + \mathcal{O}(1/\tan\beta), \qquad p = \mu_0^2, m_0^2, m_{1/2}^2, A_0^2, B_0^2. \qquad (8)$$

This is showing that one-loop corrections to the quartic coupling reduce the amount of fine-tuning significantly. In fact it is the smallness of the quartic Higgs coupling (fixed in the MSSM by gauge interactions) that is at the origin of substantial tree-level fine tuning. That this is so can be seen from the relation $v^2 \sim -m_i^2/\lambda$ where v is of $\mathcal{O}(100)$ GeV, $m_i \sim \mathcal{O}(TeV)$ while at the same time $\lambda < 1$, which makes it difficult to separate the EW and SUSY breaking

[4]The radiative corrections to couplings λ_j and soft masses m_i bring about additional field dependence, and therefore additional v and β dependence. If we include the extra v dependence, we find the fine-tuning Δ_p changes into $\Delta_p^{'} = \Delta_p/(1 - \Delta_{v^2})$ with Δ_{v^2} *defined* by eq.(6). $|\Delta_{v^2}| \ll 1$ in most cases examined. We do not include this effect here and work with Δ defined by eqs.(4), (6).

scales (for a discussion see [7]). Loop corrections increase the quartic couplings and in most cases reduce the overall amount of fine tuning.

For a general two-Higgs doublet model formulae (4), (6) can be expressed in terms of only derivatives of couplings and of masses wrt to the corresponding parameter, see Appendix in [17] (also Appendix A.1). For the CMSSM we use this result, in which we consider the full two-loop (leading log) corrections to the quartic couplings and masses. This defines unambiguously our procedure for evaluating the EW fine-tuning in CMSSM.

3 Electroweak fine tuning and its effects on the Higgs mass

In the following, the numerical results we present for Δ include two-loop corrections with:

• radiative electroweak breaking (EWSB),

• non-tachyonic SUSY particle masses (avoiding colour and charge breaking (CCB) vacua).

• experimental constraints considered: bounds on superpartner masses, electroweak precision data, $b \to s\,\gamma$, $b \to \mu\,\mu$ and anomalous magnetic moment δa_μ, as detailed in Table 1.

• consistency of m_h with the LEPII bound (114.4 GeV) and/or consistency with thermal relic density constraint, only if stated explicitly.

Constraint	Reference
SUSY particle masses	Routine in MicrOmegas 2.2, "MSSM/masslim.c"
$\delta a_\mu < 366 \times 10^{-11}$	PDG (sys. and stat. 1σ errors added linearly)
$3.20 < 10^4\ \mathrm{Br}(b \to s\gamma) < 3.84$	PDG (sys. and stat. 1σ errors added linearly)
$\mathrm{Br}(b \to \mu\mu) < 1.8 \times 10^{-8}$	Particle Data Group
$-0.0007 < \delta\rho < 0.0012$	Particle Data Group

Table 1: Constraints tested using MicrOMEGAs 2.2 with SuSpect 2.41 spectrum calculator. Particle Data Group: http://pdg.lbl.gov/.

Using these constraints we evaluated Δ numerically. The LEPII bound on the mass of the Higgs provides an important constraint for the MSSM since it requires quantum corrections in order to be satisfied. Large quantum corrections need in turn large soft masses, which in turn trigger large fine-tuning. This is seen from the loop corrections to m_h which give a strong exponential dependence on m_h, $\Delta \sim m_0^2 \sim \exp(m_h^2/m_{top}^2)$. To examine this dependence in detail, in the following we choose to present the numerical results as a function of m_h. Unless

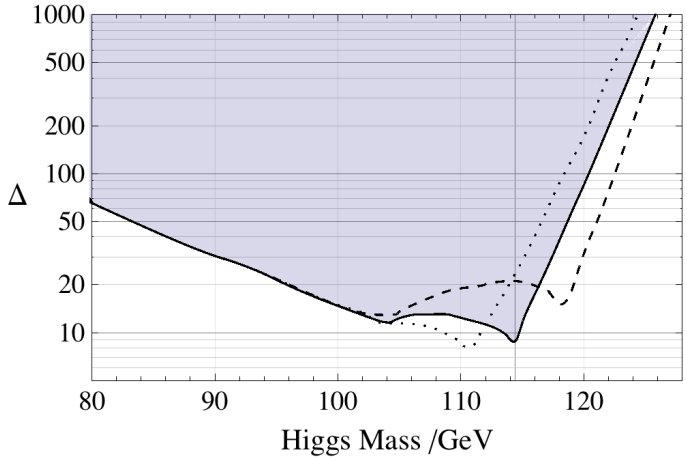

Figure 1: Fine tuning vs Higgs mass, in a two-loop analysis. The data points are for $2 \leq \tan\beta \leq 55$. The solid line is the minimum fine tuning with central values $(\alpha_3, m_t) = (0.1176, 173.1\,\text{GeV})$. The dashed line corresponds to $(\alpha_3, m_t) = (0.1156, 174.4\,\text{GeV})$ and the dotted line to $(0.1196, 171.8\,\text{GeV})$, to account for 1σ experimental errors in α_3 and top mass [34]. This is the "worst" case scenario, when such deviations combine such as to give the largest variation of Δ. An increase of $\alpha_3(m_Z)$ or reduction of $m_t(m_Z)$ by 1σ have similar effects, which can be also understood from the relation between the mass of top evaluated at m_Z and at m_t. Keeping either α_3 or m_t fixed to its central value and varying the other within 1σ brings a curve situated half-way between the continuous line and the corresponding dashed or dotted line. The LEPII bound of 114.4 GeV is indicated by a vertical line. Note the steep ($\approx$ exponential) increase of Δ on both sides of its minimum value situated near the LEPII bound.

stated otherwise, the LEPII bound on m_h is not imposed. The relic density constraint is imposed only after all the constraints other than the LEPII bound on m_h are satisfied and, when done, this is stated explicitly.

Before proceeding to present our numerical results obtained with the above constraints, let us mention the details of the procedure followed. First the fine-tuning is evaluated at two-loop order, including the dominant third generation supersymmetric threshold effects to the scalar potential. The scan is done over all parameter space using a slightly simplified two-loop calculation performed by a Mathematica code, based on the formulae in the Appendix, and optimised to run quickly. For the points in phase space that have the smallest fine-tuning (say with $\Delta < 1000$), the analysis is re-done using (the slower) SOFTSUSY 3.0.10 [29] that includes all the two-loop radiative effects mentioned. This two-step procedure is extremely important, since otherwise the CPU run time using SOFTSUSY alone would be about 6 years (when run on 30 parallel processors at 3GHz each), which prevented previous investigations at this precision level. Our two-loop analysis is also important because there is a significant

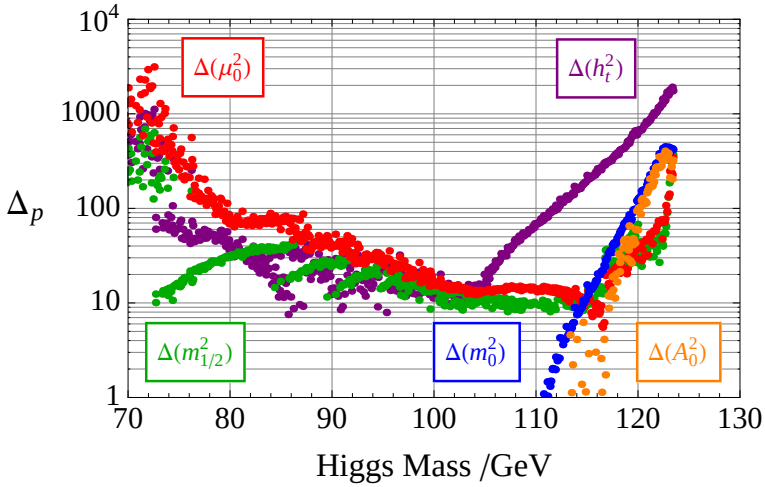

Figure 2: The plot displays the various contributions $\max|\Delta_p|$, $p = \mu_0^2, m_0^2, A_0^2, B_0^2, m_{1/2}^2$, to the electroweak fine-tuning Δ presented in Figure 1. The largest of these for all m_h gives the curve presented in Figure 1. At low m_h, $\Delta_{\mu_0^2}$ (red) is dominant, while at large m_h, $\Delta_{m_0^2}$ (blue) is dominant (with $\Delta_{A_0^2}$ reaching similar values near 120 GeV). The transition between the two regions is happening at about 114.5 GeV. Note that in this plot the LEPII bound is not imposed at any time. Although $\Delta_{h_t^2}$ (purple) is presented above for illustration, this contribution is always sub-dominant when assuming the modified definition of fine-tuning [26], appropriate for measured parameters (as we do in the text).

difference between one-loop and two-loop values for overall Δ, and was not performed in the past. QCD effects can compete at two-loop with Yukawa couplings effects, can dominate them and also displace the minimum of the fine tuning from its one-loop value. Regarding the Higgs mass, its value computed with SOFTSUSY agrees with that found using SuSpect [30] within 0.1 GeV, but can differ by ± 2 GeV [31] from the value found using FeynHiggs [32]. We use the SOFTSUSY Higgs mass for all figures in the paper. Given the small discrepancy with FeynHiggs, coming from higher order terms in the perturbative expansion, the LEPII bound should be interpreted as $m_h > 114.4 \pm 2$ GeV. In the following analysis the results are always quoted with respect to the central value of m_h.

Turning now to the numerical results, Figure 1 presents the two-loop result for the dependence of overall electroweak fine tuning Δ as a function of the Higgs mass. The dark matter constraint and the LEPII bound on m_h are not included. The loop effects reduce the fine tuning amount; the dominant effects come from quantum corrections to the quartic couplings (rather than to soft masses), which are increased by radiative effects and thus reduce Δ. Δ is seen to have a minimum close to the LEPII bound of m_h. The individual contributions to Δ are shown in Figure 2. Below the LEPII bound, detailed calculations show that the

minimal value of Δ is dominated by $\Delta_{\mu_0^2}$ and this increases rapidly for decreasing m_h. For values of m_h above the LEPII bound, Δ is dominated by[5] $\Delta_{m_0^2}$. This happens at the edge of the focus point region. The transition from the dominant $\Delta_{\mu_0^2}$ regime to the dominant $\Delta_{m_0^2}$ regime occurs near the LEPII bound value, and this is the point where the QCD radiative effects become important. This can be seen from Figure 1 where an increase by 1σ of α_3 corresponds to a larger Δ for a same, fixed value of m_h. In this sense one could even say that the minimal value of Δ is situated at the transition region between dominant effects, Yukawa versus QCD interactions. Away from the minimum of Δ, fine tuning increases dramatically, roughly exponentially. This is because, as discussed above, Δ depends exponentially on m_h.

In conclusion, the fine tuning at two-loop with all the latest constraints is minimised for

$$\Delta \approx 8.8, \qquad m_h = 114 \pm 2 \text{ GeV} \tag{9}$$

with the theoretical uncertainty of ± 2 GeV, explained earlier.

Note that our analysis also investigated the contribution to Δ coming from the uncertainty in measured "parameters" such as top Yukawa and strong coupling. Using the modified[6] definition [26], appropriate for measured parameters, we find their fine-tuning is sub-dominant.

Finally, let us also mention that the reduction of fine-tuning that we have seen is mostly due to (two-) loop corrections considered, particularly to quartic couplings and is actually very significant, given the conservative scenario considered here assuming universal gaugino mass structure of the CMSSM; relaxing this condition could reduce [6] Δ further.

3.1 Constraints on Δ from fixing $\tan\beta$

It is interesting to examine the fine-tuning for fixed values of some of the parameters present, to see the individual impact of such constraints on Δ. Here we do this for a fixed value of $\tan\beta$. This is shown[7] in Figure 3 for increasing vales of $\tan\beta$, with $\tan\beta = 2$ (blue), $\tan\beta = 3$ (red), $\tan\beta = 10$ (green). Increasing $\tan\beta$ shifts the curves of Δ towards larger m_h and, to a limited extent, to lower fine-tuning, reached for medium $\tan\beta \sim 10$, also for larger $\tan\beta \sim 40$ (see later, Fig.7 (a)). As may be seen from the figure, the two-loop expressions for soft masses

[5] Larger m_h requires larger $m_{\tilde{t}}^2 \sim m_0^2$, and a larger m_0, above the focus point region, increases $\Delta_{m_0^2}$.

[6] $\bar{\Delta}_p = \Delta_p \times (\sigma_p/p)$ where σ_p is the 1σ error in the parameter p derived from experimental observation.

[7] In Figures 3, 4, 5 only, Δ is computed with our Mathematica code instead of SOFTSUSY, due to long CPU time constraints. This explains the small difference in shape between the two-loop line in these three figures from the more accurate one in Figure 1 and all other figures (based on SOFTSUSY).

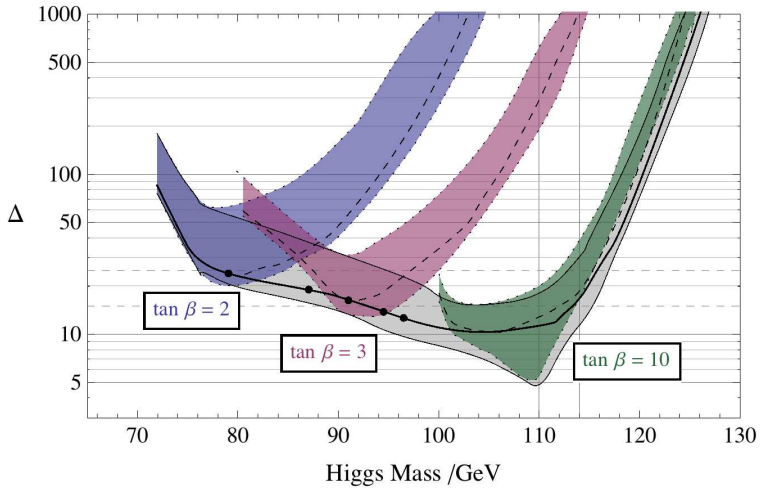

Figure 3: Minimum fine tuning versus Higgs mass at two-loop, showing the influence of loop effects and $\tan\beta$ on fine tuning. All constraints listed in Table 1 are included. The upper and lower lines associated with the coloured regions are the 1-loop without thresholds for λ and soft masses and "full" 1-loop results respectively (similarly for the grey region, for all $\tan\beta$). The minimum 2-loop fine tuning is found between these two cases. The solid lines refer to the scan $2 \leq \tan\beta \leq 55$. The black points give the positions of minimum Δ for fixed $\tan\beta$ from 2 to 4 inclusive in steps of 0.5.

and couplings bring values of Δ which are situated between the higher "tree-level" curve (i.e. tree-level for λ_i, one-loop for soft masses without field dependent threshold effects) and the lower one-loop case (one-loop for both λ_i and soft masses). This is consistent with what one would expect from a convergent, perturbative, loop expansion. The roughly exponential behaviour of Δ at large m_h for fixed $\tan\beta$ can bring a significant variation of Δ.

3.2 Constraints on Δ from the SUSY spectrum

Here we examine the impact on Δ due to constraints related to the supersymmetric spectrum. The key features of the impact of this spectrum on Δ can be seen from the limits on the chargino mass considered in Figure 4. Currently, the (lightest) chargino mass bound is the most important, followed by that of the neutralino. It also turns out that the gluino mass limit is not very constraining. These results follow recent experimental data, since using the 1998 data it was the neutralino mass bound that was more constraining for Δ.

In Figure 4, the effect of the chargino mass $m_{\chi_1} > 94$ and $m_{\chi_1} > 80$ GeV is shown by the upper and lower continuous curves. While these can have some impact on fine-tuning for values of m_h already ruled out experimentally, for $m_h > 114.4$ GeV, the effect is overlapping

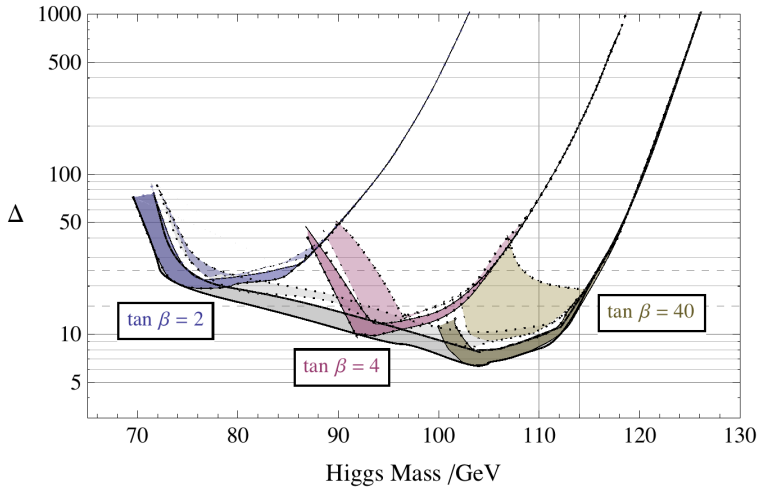

Figure 4: Minimum fine tuning vs Higgs mass, showing the influence of mass constraints on fine tuning. The results are at 2-loop with the upper shaded (coloured) areas connecting the case of only applying the SUSY spectrum constraints (lower line) to that with all constraints listed in Table 1 (upper line). The lower shaded (coloured) areas connect the cases of only applying a chargino lower mass limit of 80 and 94 GeV for the lower and upper lines respectively. The results for the scan $2 \leq \tan\beta \leq 55$ are also shown by the grey shaded area, with similar convention for upper/lower continuous lines delimiting it.

that from $b \to s\gamma$ (see later). Further, the close vicinity of the upper and lower dotted curves corresponding to all constraints in Table 1 and to the SUSY spectrum limits respectively shows that the latter are the main constraints at the moment for Δ at low $\tan\beta$. The graph presents Δ and m_h computed using quartic couplings and mass expressions evaluated at two-loop.

3.3 Constraints on Δ from $b \to s\gamma$

Figure 5 gives the impact of the $b \to s\gamma$ constraint on Δ. The lower limit of the $b \to s\gamma$ constraint for a given coloured area (fixed $\tan\beta$) restricts the right hand edges of the plot, while the upper limit restricts its left hand side. These curves also depend on the mass limits - these constraints are not fully independent. For the experimentally allowed area of $m_h > 114.4$ GeV, the impact of the constraint $b \to s\gamma$ is rather small; in this case its effect is overlapping that of the SUSY mass limits, as can be seen from the rhs of the plots for individual $\tan\beta$ plots. The combination of the SUSY mass limits and $b \to s\gamma$ constraint currently dominate the restriction on how small the fine tuning could be, see also Figure 6. In this last figure one can easily see, at two-loop, the impact on Δ of removing the $b \to s\gamma$ constraint. For a related analysis of $b \to s\gamma$ see recent [27].

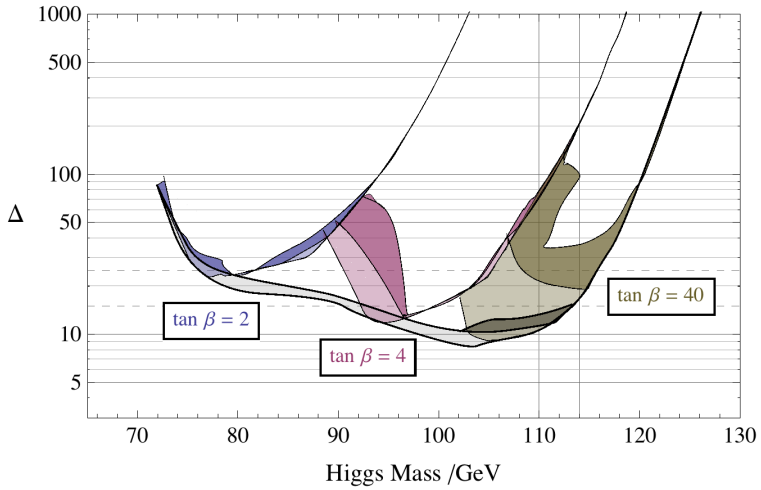

Figure 5: Minimum fine tuning vs Higgs mass, showing the influence of the $b \to s\gamma$ constraint. The results are at 2-loop with the lighter shading connecting the case of only applying the SUSY spectrum constraints (lower line) to that with also the $b \to s\gamma$ constraint listed in Table 1 (upper line). This upper edge of this shading is indistinguishable from the solid line which includes all constraints in Table 1. The darker shading extends up to the minimum fine tuning limits for the case, $3.52 < 10^4\,\mathrm{Br}(b \to s\gamma) < 3.77$, with the other constraints as given in Table 1. The results for the scan $2 \leq \tan\beta \leq 55$ are also shown, between the two continuous and almost parallel lower curves.

The other constraints listed in Table 1 do eliminate further mSUGRA points, but have a negligible effect on the fine tuning limits. With the current mass limits, a change in the δa_μ constraint by factors of 2 or more does not affect these results significantly.

3.4 Constraints on Δ and the CMSSM parameters

The fine tuning measure can be easily applied to establish the remaining allowed range for the MSSM SUSY parameters. In Figure 7 we plotted the dependence of the total fine tuning wrt various parameters. To understand some aspects of the dependence of the electroweak scale fine tuning on the MSSM parameters, let us use, for the sake of discussion, one of the two minimum conditions which, when ignoring quantum corrections to quartic couplings, simplifies to:

$$\frac{m_Z^2}{2} \;=\; \frac{m_1^2 - m_2^2\tan^2\beta}{\tan^2\beta - 1} \tag{10}$$

Using 2-loop RGE solutions at $\tan\beta = 10$ (for details see the Appendix), one has

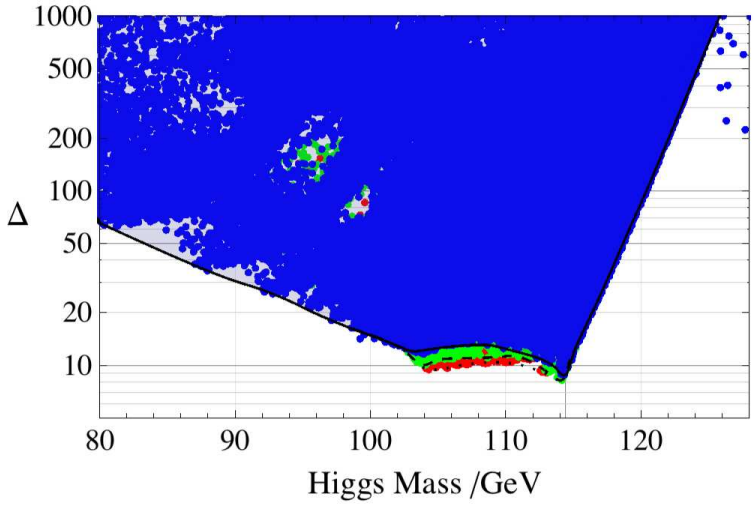

Figure 6: Minimum fine tuning vs Higgs mass, showing the influence of the $b \to s\gamma$ constraint. In the presence of this constraint with 3σ limits, the red (lower) region is removed. Within the 1σ limits, the green (middle) band is removed leaving the blue (upper) points. This is a two-loop leading log approximation, obtained using SOFTSUSY.

$$m_1^2(m_Z) \approx 0.99\,\mu_0^2 + 0.946\,m_0^2 + 0.331\,m_{1/2}^2 + 0.044\,A_0\,m_{1/2} - 0.013\,A_0^2 \quad (11)$$

$$m_2^2(m_Z) \approx 0.99\,\mu_0^2 - 0.080\,m_0^2 - 2.865\,m_{1/2}^2 + 0.445\,A_0\,m_{1/2} - 0.099\,A_0^2 \quad (12)$$

It is the large cancellation between the μ_0^2 and $m_{1/2}^2$ terms that is often responsible for the large fine tuning (note however that this argument ignores the impact of quantum corrections to quartic couplings, known to reduce the fine-tuning). This leads to the approximate relation $\Delta_{\mu_0^2} \sim \Delta_{m_{1/2}^2}$. As low fine tuning prefers small μ_0, small $m_{1/2}$ is also preferred and this is observed in Fig 7 (e), (f). The rise in fine tuning at small $m_{1/2}$ is a consequence of the constraints such as the chargino mass limit.

The near flat distribution of minimum fine tuning in m_0 is a result of the coefficient of m_0 in m_2 being driven close to zero. The fine tuning with respect to m_0 then rarely dominates, until we reach values of m_h above the LEPII bound (m_0 at the edge of focus point region). The result of applying the Higgs mass constraint also excludes a region with small $m_{1/2}$ at m_0 below 1.5 TeV. The focus point at $m_0 \sim 1.5$ TeV where the minimum of $m_{1/2}$ is possible, corresponds to the point where fine tuning is minimised. This only occurs for large $\tan\beta$, and this available "dip" in fine tuning in the mSUGRA space disappears as $\tan\beta$ is reduced.

Figure 7(c) indicates that a small trilinear coupling $|A_0| \lesssim 1$ TeV is preferred for the smallest fine tuning. This follows from a similar argument for preferring small $m_{1/2}$. Increasing

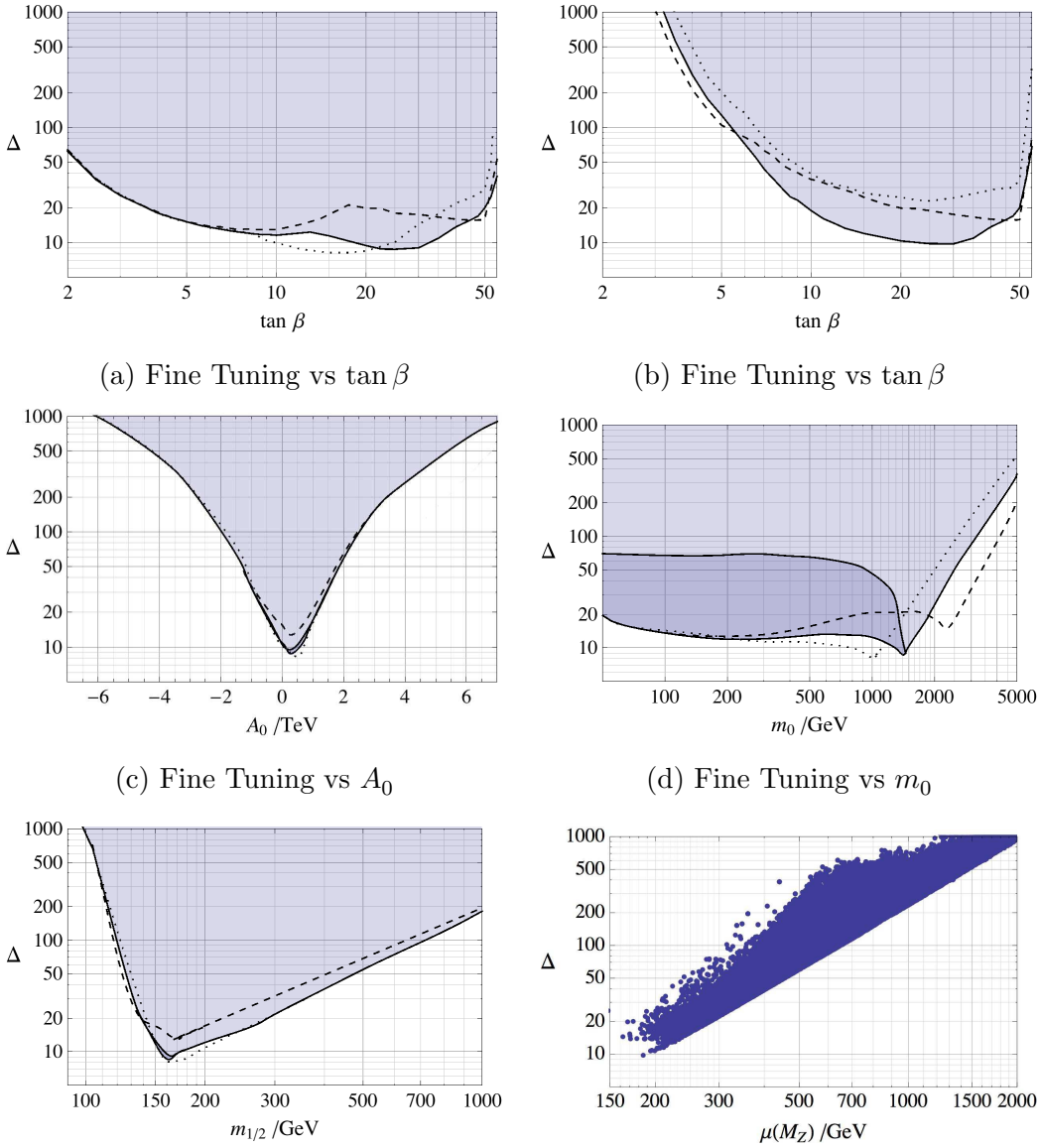

(a) Fine Tuning vs $\tan\beta$

(b) Fine Tuning vs $\tan\beta$

(c) Fine Tuning vs A_0

(d) Fine Tuning vs m_0

(e) Fine Tuning vs $m_{1/2}$

(f) Fine Tuning vs μ

Figure 7: Dependence of minimum fine tuning on SUSY parameters ($\mu > 0$, relic density unrestricted). The solid, dashed and dotted lines are as explained in Fig 1. No bound on m_h is applied in figure (a). In (c), (d), (e), the darker shaded regions are eliminated when $m_h > 114.4$ GeV is applied for the case with the central (α_3, m_t) values. In (b) and (f), $m_h > 114.4\,\text{GeV}$ is applied, and the points in (f) are only for the central (α_3, m_t) values.

$|A_0|$ requires larger cancellations with μ to set the electroweak scale. However, once the Higgs mass constraint is applied, A_0 is driven negative for small $\tan\beta$ in order to maximise the

stop mixing. The related increase in the minimum fine tuning from being in this region of parameter space then follows. This is important for small $\tan\beta$ where the tree level Higgs mass is smallest. The sign structure of the UV parameter coefficients in m_2 leads to a preference in a small, positive A_0.

As mentioned earlier, the fine tuning measure Δ can be used to establish the remaining parameter space of the CMSSM compatible with a solution to the hierarchy problem. Assuming that $\Delta = 100$ is the upper limit beyond which we consider that SUSY failed to solve the hierarchy problem, we obtain the following bounds:

$$\begin{array}{rcl@{\qquad}rcl} m_h & < & 121 \text{ GeV} & 5.5 < & \tan\beta & < 55 \\ \mu & < & 680 \text{ GeV} & 120 \text{ GeV} < & m_{1/2} & < 720 \text{ GeV} \\ m_0 & < & 3.2 \text{ TeV} & -2.0 \text{ TeV} < & A_0 & < 2.5 \text{ TeV} \end{array} \tag{13}$$

These values can be easily re-calculated for a different value of Δ.

3.5 Constraints on Δ from the relic density

It is interesting to see the impact on Δ and on the CMSSM parameters from the presence of the dark matter relic density constraint (examined using micrOMEGAs2.2 [35]) and the LEPII constraint on m_h. These are rather strong constraints, particularly in the "restrictive" context of CMSSM that we study, with universal gaugino mass. The results are presented in Figure 8, where the relative impact of the LEPII constraint can be seen by comparing the left and right plots. If the observed dark matter abundance is imposed as a constraint on the CMSSM, then the range of values given in (13) and valid for $\Delta < 100$ is further restricted, as seen in Figure 8. The condition that the SUSY LSP should provide the observed dark matter abundance as well as the constraint $m_h > 114.4$ GeV removes the intermediate values of $m_{1/2}$ and m_0, but has a rather small impact on A_0.

3.6 Prediction for m_h from minimising Δ and saturating the relic density

The relic density constraint can be combined with that of minimal electroweak fine-tuning Δ to make an interesting prediction for m_h. Figure 9 shows the impact of non-baryonic relic density constraint on Δ presented in Figure 1. Obviously, not all initial points in Δ satisfy this constraint, and this is shown in Figure 9 by the red and blue points which do not fill the whole area above the continuous line of minimal Δ. As expected, the additional dark

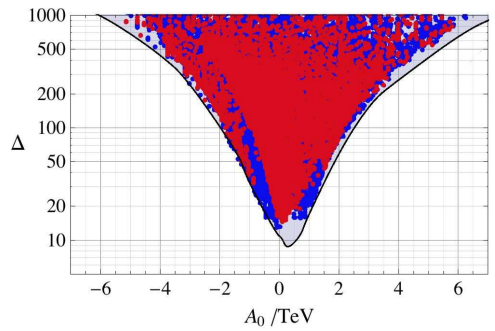

(a) Fine tuning vs A_0

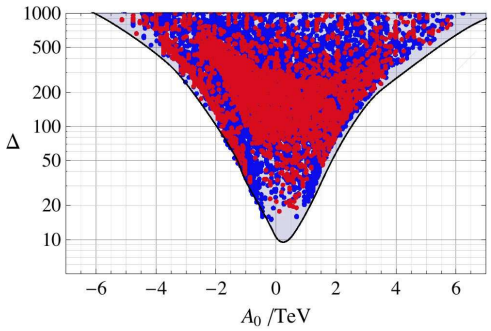

(b) Fine tuning vs A_0, $m_h > 114.4$GeV

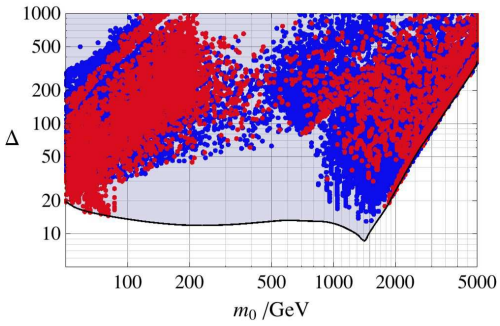

(c) Fine tuning vs m_0

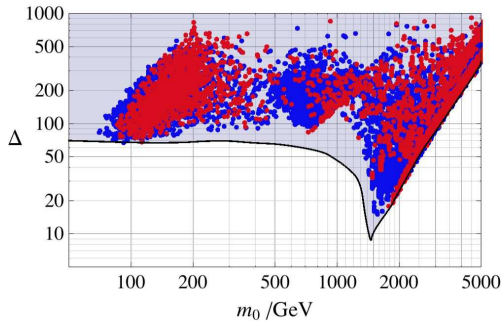

(d) Fine tuning vs m_0, $m_h > 114.4$ GeV

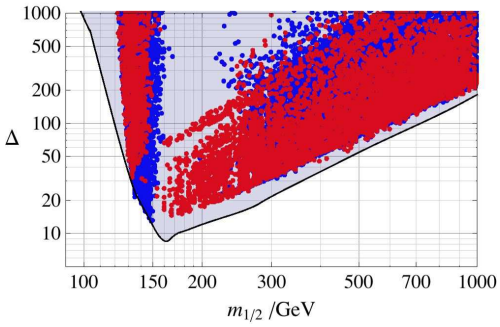

(e) Fine tuning vs $m_{1/2}$

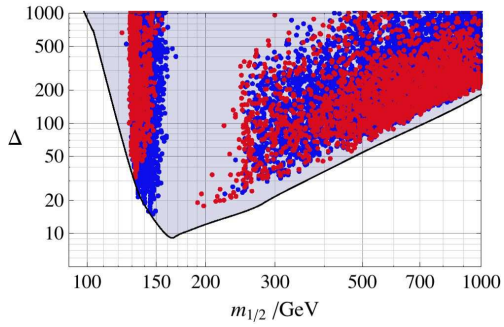

(f) Fine tuning vs $m_{1/2}$, $m_h > 114.4$ GeV

Figure 8: Dependence of minimum fine tuning on SUSY parameters, with the relic density saturated within 3σ of the WMAP bound (in red). The WMAP bound is $\Omega h^2 = 0.1099 \pm 0.0062$ [33]. The blue (darker) points do not saturate the relic density $\Omega h^2 \leq 0.0913$ (3σ deviation). The impact of the constraint $m_h > 114.4$ GeV is also considered. Compare this figure to Figure 7 where relic density constraint was not included. The parameters values quoted in eq.(13) are further restricted, as seen from these plots. The continuous line is that of minimal electroweak Δ (no relic density constraint).

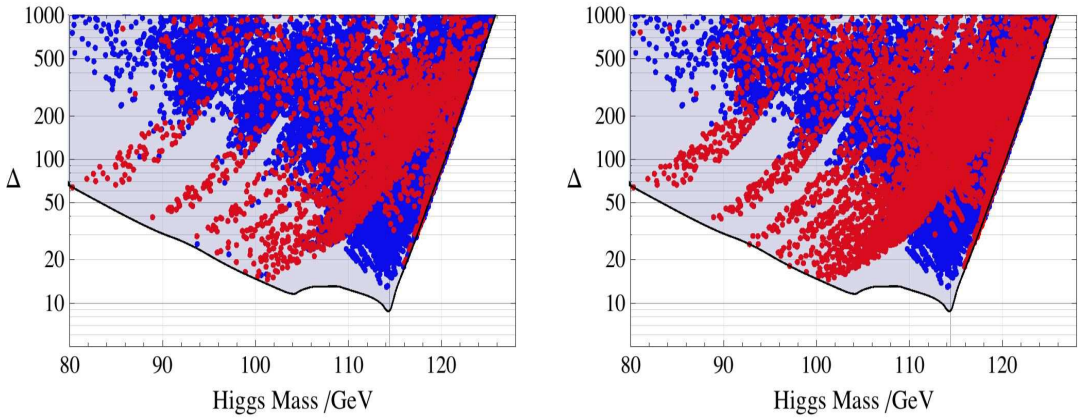

Figure 9: Fine tuning vs Higgs mass with the influence of the WMAP bound. The minimum fine tuning at 2-loop for $2 \leq \tan\beta \leq 55$ is given by the solid line when including all the constraints listed in Table 1. Left figure: The blue (darker) points sub-saturate the relic density. The red (lighter) points give a relic density within the 1σ bounds, $\Omega h^2 = 0.1099 \pm 0.0062$. The 'strips' of points at low Higgs mass appear due to taking steps of 0.5 in $\tan\beta$ below 10. A denser scan is expected to fill in this region. Similarly, more relic density saturating points are expected to cover the wedge of sub-saturating points at $m_h \sim 114$ GeV and $\Delta \gtrsim 30$. Right: as for left, within 3σ WMAP bound (in red). The continuous line is that of minimal electroweak Δ without the relic density constraint.

matter constraint prefers in some cases larger Δ relative to its minimal value (continuous line) obtained only with the constraints in Table 1. However, as can be seen in the plots, the region of m_h values where this constraint is indeed relevant is actually ruled out by LEPII bound $m_h > 114.4$ GeV; above this value the two curves on the boundary are almost overlapped and the constraints in Table 1 are sufficient to also satisfy the thermal relic density; note that the red points in the left (right) plots in Figure 9 satisfy the relic density within 1σ and 3σ WMAP bounds [33], respectively. The results are obtained as usual, using two-loop values for the quartic couplings and soft masses and corresponding threshold effects. (with the SOFTSUSY and micrOMEGAs codes).

It is important to notice that, *without* imposing the LEPII bound, at the two-loop level, the smallest fine tuning Δ consistent with the relic density WMAP bounds [33] predicts a mass for the lightest Higgs as follows:

$$\begin{aligned} m_h &= 114.7 \pm 2 \text{ GeV}, \quad \Delta = 15.0, \quad \text{(sub-saturating the WMAP bound)}. \\ m_h &= 116.0 \pm 2 \text{ GeV}, \quad \Delta = 19.1, \quad \text{(saturating the WMAP within } 1\sigma\text{)}. \\ m_h &= 115.9 \pm 2 \text{ GeV}, \quad \Delta = 17.8, \quad \text{(saturating the WMAP within } 3\sigma\text{)}. \end{aligned} \tag{14}$$

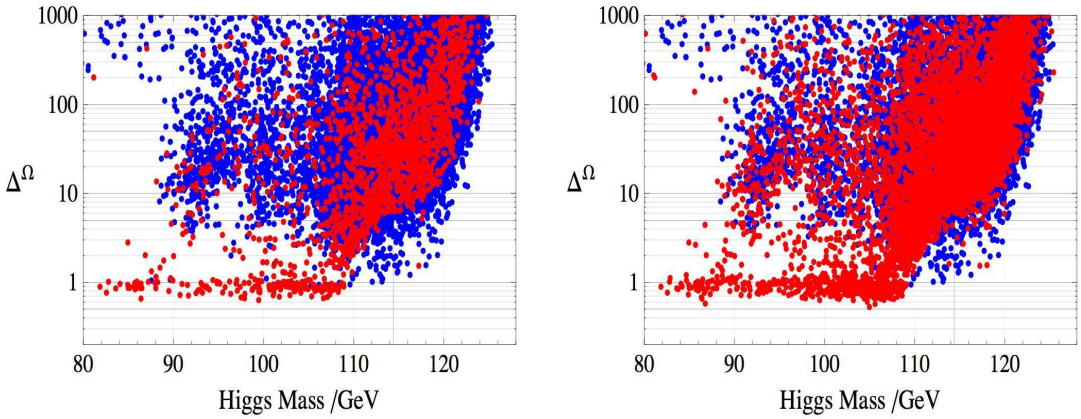

Figure 10: Left (Right) figure: Relic density fine tuning, Δ^Ω in function of the Higgs mass, at two-loop level, for a 1σ (3σ) WMAP bound (red), respectively. The blue (darker) points sub-saturate the dark matter relic density.

To conclude, minimising the fine-tuning together with the constraints from precision electroweak data, the bounds on SUSY masses and the requirement of the observed dark matter abundance lead to a prediction for m_h, without imposing the LEPII bound. This is an interesting result, and represents our prediction for the CMSSM lightest Higgs mass based on assuming Δ as a quantitative test of SUSY as a solution to the hierarchy problem.

4 Dark matter fine tuning and its effect on the Higgs mass

The dark matter abundance can be very sensitive to the choice of parameters and can introduce a new fine tuning to the model. To quantify this it is interesting to consider the dark matter fine tuning Δ^Ω wrt the CMSSM parameters, and to determine its impact on the overall fine tuning (for earlier studies see [15, 16] and references therein). Its definition is similar to that of Δ:

$$\Delta^\Omega = \max \left| \frac{\partial \ln \Omega h^2}{\partial \ln q} \right|_{q=m_0, m_{1/2}, A_0, \tan\beta} \tag{15}$$

In Figure 10 we evaluated Δ^Ω at two-loop level and presented as a function of the Higgs mass, without imposing any restriction on the latter. It turns out that Δ^Ω can have acceptable values even for m_h close to 120 GeV. In Figure 11 the total fine-tuning, defined as $\max\{\Delta, \Delta^\Omega\}$ is presented as a function of m_h. Its value is only slightly larger than that found earlier for

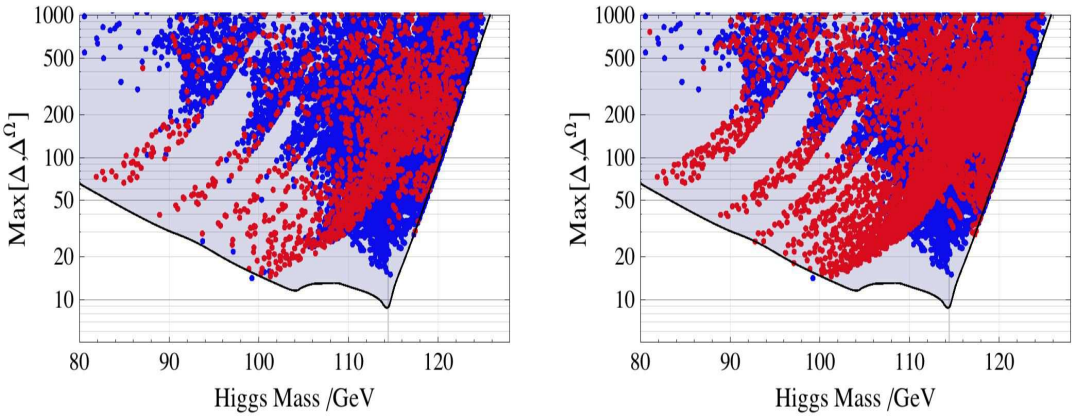

Figure 11: Left (Right) figure: The total fine tuning, $\max\{\Delta, \Delta^{\Omega}\}$ in function of the Higgs mass, at two-loop level, for a 1σ (3σ) WMAP bound (in red), respectively. The blue (darker) points sub-saturate the dark matter relic density. The continuous line represents the minimal value of the EW fine-tuning computed earlier.

Δ alone with WMAP saturated dark matter abundance (in red in the plots). From Figure 11 we predict, from minimising $\max\{\Delta, \Delta^{\Omega}\}$ and from consistency with the 3σ WMAP bound:

$$\begin{aligned} m_h &= 114.70 \pm 2 \text{ GeV}, \ \max\{\Delta, \Delta^{\Omega}\} = 15, \quad \text{(sub-saturating WMAP bound)} \\ m_h &= 116.98 \pm 2 \text{ GeV}, \ \max\{\Delta, \Delta^{\Omega}\} = 28.7, \ \text{(saturating WMAP bound within } 3\sigma) \end{aligned} \tag{16}$$

The last predicted value of m_h is only marginally above that predicted in (14), based on minimised electroweak fine-tuning and right dark matter abundance.

5 Predictions for the superpartners from fine tuning limits

The results so far demonstrate that electroweak fine-tuning has a strong sensitivity to parameters such as μ, $m_{1/2}$, with a preference for lower values. Regarding the m_0 dependence, Δ has a rather flat dependence when we are in the focus point region. The states that are dominantly controlled by the μ, $m_{1/2}$ parameters are then the most important in determining the naturalness of the proposed theory. These include the neutralinos, charginos and the gluino states. Further, setting an upper bound on electroweak Δ gives a bound on the spectrum. If any of these states have masses in excess of those given in Table 2, it will require less than 1% tuning ($\Delta > 100$) for the MSSM.

$\tilde{g}$	χ_1^0	χ_2^0	χ_3^0	χ_4^0	$\chi_1^\pm$	$\chi_2^\pm$	$\tilde{t}_1$	$\tilde{t}_2$	$\tilde{b}_1$	$\tilde{b}_2$
1720	305	550	660	665	550	670	2080	2660	2660	3140

Table 2: Upper mass limits on superpartners in GeV such that $\Delta < 100$ remains possible.

These upper mass limits scale approximately as $\sqrt{\Delta_{\rm min}}$, so they may be adapted depending on how much fine tuning the reader is willing to accept. Overall low fine tuning prefers a Higgsino mass of $\mathcal{O}(0.5$ TeV), a gluino of $\mathcal{O}(1.5$ TeV) and chargino and neutralino masses of $\mathcal{O}(300$ GeV). Stop and sbottom masses are significantly larger at $\mathcal{O}(3$ TeV) due to the weak limit on m_0 (focus point).

Finally we return to the intriguing fact that minimum electroweak fine tuning plus correct dark matter abundance corresponds to a Higgs mass just above the LEPII bound[8]. As we noted above this point is fixed by the current bounds on the SUSY spectrum and not by the current Higgs mass bound which is not included when doing the scans giving Figs 1, 2, 9, 11.

One may interpret the SUSY parameters corresponding to this point as being the most likely given our present knowledge and so it is of interest to compute the SUSY spectrum for this parameter choice as a benchmark for future searches. This is presented in Table 3 where it may be seen that it is somewhat non-standard with very heavy squarks and sleptons and lighter neutralinos, charginos and gluinos. This has similarities to the SPS2 scenario [36].

5.1 Predictions for SUSY searches at the LHC

It is clear that there is still a wide range of parameters that needs to be explored when testing the CMSSM. Will the LHC be able to cover the whole range? To answer this note that, for a fine tuning measure $\Delta < 100$, one must be able to exclude the upper limits of the mass parameters appearing in Table 2. Of course the state that affects fine tuning most is the

[8]One may ask whether the fine-tuning measure used above has indeed a clear physical meaning. One can object that nature may not choose "minimal" fine-tuning results. One can invoke the example of *classical* chaotic systems, displaying the familiar "butterfly effect" where small variations of the initial conditions bring large changes of the final state ("fine tuning"), yet the system is "realised". Such effects exist in (nonlinear) classical systems, where initial close values (states) of a parameter exponentially diverge after evolving according to the dynamics of the differential eqs. In our setup, one could have such effects not from evolution in time but from evolution wrt the energy scale, from the high scale to the low scale, after including *quantum* effects encoded in the RG differential equations. By this analogy one could object that using criteria of low fine-tuning to obtain mass bounds (for m_h) may not be appropriate. However, the difference is that the discussion in the text is at *quantum level*, so the counterexamples of *classical* (chaotic) systems do not necessarily apply.

h^0	114.5	$\tilde{\chi}_1^0$	79	$\tilde{b}_1$	1147	$\tilde{u}_L$	1444
H^0	1264	$\tilde{\chi}_2^0$	142	$\tilde{b}_2$	1369	$\tilde{u}_R$	1446
$H^\pm$	1267	$\tilde{\chi}_3^0$	255	$\tilde{\tau}_1$	1328	$\tilde{d}_L$	1448
A^0	1264	$\tilde{\chi}_4^0$	280	$\tilde{\tau}_2$	1368	$\tilde{d}_R$	1446
$\tilde{g}$	549	$\tilde{\chi}_1^\pm$	142	$\tilde{\mu}_L$	1406	$\tilde{s}_L$	1448
$\tilde{\nu}_\tau$	1366	$\tilde{\chi}_2^\pm$	280	$\tilde{\mu}_R$	1406	$\tilde{s}_R$	1446
$\tilde{\nu}_\mu$	1404	$\tilde{t}_1$	873	$\tilde{e}_L$	1406	$\tilde{c}_L$	1444
$\tilde{\nu}_e$	1404	$\tilde{t}_2$	1158	$\tilde{e}_R$	1406	$\tilde{c}_R$	1446

Table 3: The favoured Constrained MSSM spectrum of minimal $\Delta = 15$ giving a sub-saturation of the WMAP bound. Masses are given in GeV.

Higgs scalar and one may see from Figure 1 that establishing the bound $m_h > 120\,\text{GeV}$ will imply that $\Delta > 100$. However the least fine tuned region corresponds to the lightest Higgs consistent with the LEPII bound and this is the region where the LHC searches rely on the $h \to \gamma\gamma$ channel which has a small cross section and will require some $30\,fb^{-1}$ at $\sqrt{s} = 14\,\text{TeV}$ to explore. Given this it is of interest to consider to what extent the direct SUSY searches will probe the low fine tuned regions. Following the discussion in the previous section, the most significant processes at the LHC will be those looking for gluinos, winos and neutralinos.

Studies of SUSY at the LHC [37] have shown that the LHC experiments have a sensitivity to gluinos of mass 1.9 TeV for $\sqrt{s} = 10\,\text{TeV}$, 2.4 TeV for $\sqrt{s} = 14\,\text{TeV}$ and luminosity $10 fb^{-1}$. Of relevance to the first LHC run the limit is 600 GeV for $\sqrt{s} = 10\,\text{TeV}$ and luminosity $100\,pb^{-1}$. These correspond to probing up to $\Delta = 120, 180$ and 14 respectively. As we have discussed charginos and neutralinos can be quite light, but their signal events are difficult for LHC to extract from the background, owing in part to a decreasing $M_{\widetilde{W}} - M_{\widetilde{Z}}$ mass gap as $|\mu|$ decreases [38, 39]. An Atlas study [40] of the trilepton signal from chargino-neutralino production found that $30 fb^{-1}$ luminosity at 14 TeV is needed for a 3σ discovery significance for $M_2 < 300$ GeV and $\mu < 250$ GeV [41].

6 Summary and Conclusions

Supersymmetry was introduced to solve the hierarchy problem and to avoid the large fine-tuning in the SM Higgs sector associated with the Planck or GUT scale when quantum corrections are included. While this hierarchy problem is solved by TeV-scale supersymmetry,

the non-observation, so far, of SUSY states means that the MSSM has acquired some residual amount of fine-tuning related to unnatural cancellations in the SUSY breaking sector. The goal of this paper was to analyse in detail the level of fine tuning in the CMSSM.

The fine tuning measure Δ provides a quantitative test of SUSY as a solution to the "little" hierarchy problem and measures the "tension" required to satisfy the scalar potential minimum condition $v^2 \sim -m_{susy}^2/\lambda$, for a combination of soft masses $m_{susy}^2 \sim$ TeV, with an effective quartic coupling $\lambda < 1$ and $v \sim \mathcal{O}(100)$ GeV. Although the exact upper limit on the fine tuning Δ beyond which a theory fails to solve the hierarchy problem is debatable, it is preferable, for a given model, to have a parameter space configuration corresponding to the lowest value of Δ. We evaluated Δ at two-loop order and also paid particular attention to threshold corrections and to the $\tan\beta$ radiative dependence on the parameters. Such effects on fine-tuning were not fully considered in the past and turned out to reduce fine tuning significantly.

Our determination of the fine-tuning measure for the CMSSM included the theoretical constraints (radiative EWSB, avoiding charge and colour breaking vacua), and also the experimental constraints (bounds on superpartner masses, electroweak precision data, $b \to s\,\gamma$, $b \to \mu\,\mu$ and muon anomalous magnetic moment, dark matter abundance). As far as we are aware, our study is the first two-loop analysis of the fine tuning problem in the CMSSM, largely based on SOFTSUSY and micrOMEGAs, SuSpect and our own Mathematica code. The latter was very important since it reduced to a feasible level the CPU run time necessary to scan the full parameter space.

Not including the dark matter constraint, we found the minimum value is given by $\Delta = 8.8$. Remarkably, even without imposing the LEP bound on the Higgs mass, the condition fine tuning should be a minimum predicts $m_h = 114 \pm 2$ GeV. Adding the constraint on the dark matter relic density, one finds $\Delta = 15$ corresponding to $m_h = 114.7 \pm 2$ GeV and this rises to $\Delta = 17.8$ ($m_h = 115.9 \pm 2$ GeV) for SUSY dark matter abundance within 3σ of the WMAP constraint. The results are encouraging for the search for SUSY because we considered the "conservative" case of CMSSM, and it is well-known that relaxing gaugino universality can reduce Δ further [6, 9].

The spectrum corresponding to the minimum value of the fine tuning shows similarities to the SPS2 scenario with light neutralinos, charginos and gluinos (corresponding to light μ, $m_{1/2}$) and heavy squarks and sleptons corresponding to large m_0, near the focus point

limiting value [13, 14]. It provides the "best" estimate for the SUSY spectrum given the present experimental bounds.

Increasing m_h above the minimum fine tuned value causes Δ to increases exponentially fast and one leaves the focus point region at the edge of which this minimal value is reached; one obtains $\Delta = 100$ (1000) for a scalar mass $m_h = 121$ (126) GeV, respectively. Ultimately the question whether the SUSY solution to the hierarchy problem has been experimentally tested relies on what value of fine tuning represents the limit of acceptability. Given a value one can determine the range of parameter space that is still acceptable. For the case that the fine tuning measure should satisfy $\Delta < 100$, we determined the corresponding superpartners masses and CMSSM parameters values, that can be relevant for SUSY searches.

Acknowledgements

The research was partially supported by the EU RTN grant UNILHC 23792. S.C. is supported by the UK Science and Technology Facilities Council PPA/S/S/2006/04503. D.G. thanks the Theory Group at École Polytechnique Paris for their kind hospitality and acknowledges the financial support from the ERC Advanced Grant ERC-2008-AdG 20080228 ("MassTeV"). D.G. thanks S. Pokorski for many interesting discussions on this topic.

7 Appendix

A.1 Higgs mass and EW fine tuning

We provide technical results used in the text to evaluate Δ. The potential used in (1)

$$\begin{aligned} V &= m_1^2\,|H_1|^2 + m_2^2\,|H_2|^2 - (m_3^2\;H_1\cdot H_2 + h.c.) \\ &+ \frac{1}{2}\,\lambda_1\,|H_1|^4 + \frac{1}{2}\,\lambda_2\,|H_2|^4 + \lambda_3\,|H_1|^2\,|H_2|^2 \;+ \lambda_4\,|H_1\cdot H_2|^2 \\ &+ \left[\frac{1}{2}\,\lambda_5\;(H_1\cdot H_2)^2 + \lambda_6\;|H_1|^2\,(H_1\cdot H_2) + \lambda_7\;|H_2|^2\,(H_1\cdot H_2) + h.c.\right] \end{aligned} \tag{A-1}$$

with $H_1.H_2 = H_1^0\,H_2^0 - H_1^-H_2^+$. Using the notation

$$\begin{aligned} m^2 &= m_1^2\,\cos^2\beta + m_2^2\,\sin^2\beta - m_3^2\,\sin 2\beta \\ \lambda &= \frac{\lambda_1}{2}\,\cos^4\beta + \frac{\lambda_2}{2}\,\sin^4\beta + \frac{\lambda_{345}}{4}\,\sin^2 2\beta + \sin 2\beta\left(\lambda_6\cos^2\beta + \lambda_7\sin^2\beta\right) \end{aligned} \tag{A-2}$$

the minimisation conditions give

$$v^2 = -m^2/\lambda, \qquad 2\lambda\frac{\partial m^2}{\partial\beta} = m^2\frac{\partial\lambda}{\partial\beta} \tag{A-3}$$

or, equivalently,

$$\begin{aligned} \frac{2m_3^2}{\sin 2\beta} &= m_1^2 + m_2^2 + \frac{v^2}{2}\left[\lambda_1\,c_\beta^2 + \lambda_2\,s_\beta^2 + \lambda_{345} + (\lambda_6+\lambda_7)\,s_{2\beta} + \lambda_6\cot\beta + \lambda_7\tan\beta\right] \\ m_1^2 - m_2^2\tan^2\beta &= -\frac{v^2}{2}\left[\cos^2\beta\left(\lambda_1 - \lambda_2\tan^4\beta\right) + \sin 2\beta\left(\lambda_6 - \lambda_7\tan^2\beta\right)\right] \end{aligned} \tag{A-4}$$

One finds for the CP odd Higgs mass:

$$m_A^2 = \frac{2m_3^2}{\sin 2\beta} - \frac{v^2}{2}\,(2\lambda_5 + \lambda_6\cot\beta + \lambda_7\tan\beta)\,, \qquad m_Z^2 = \frac{g^2\,v^2}{4} \tag{A-5}$$

with $g^2 = g_1^2 + g_2^2$. In the notation of [42], the CP even Higgs masses are

$$\begin{aligned} m_h^2 &= \frac{1}{2}\Big[\,m_A^2 + v^2\,(2\lambda + \Lambda_5) - \sqrt{\left[m_A^2 + v^2\,(\Lambda_5 - 2\lambda)\right]^2 + 4v^4\,\Lambda_6^2}\,\Big] \\ \Lambda_5 &= \frac{s_{2\beta}^2}{4}\,(\lambda_1 + \lambda_2 - 2\lambda_{345}) + \lambda_5 - \frac{s_{4\beta}}{2}\,(\lambda_6 - \lambda_7) \\ \Lambda_6 &= \frac{s_{2\beta}}{2}\left(\lambda_{3451}\,c_\beta^2 - \lambda_{3452}\,s_\beta^2\right) + \frac{c_{2\beta}}{2}\,(\lambda_6 + \lambda_7) + \frac{c_{4\beta}}{2}\,(\lambda_6 - \lambda_7) \end{aligned} \tag{A-6}$$

where $\lambda_{345j} = \lambda_{345} - \lambda_j$, λ is that of (2), and, $(s_\beta, c_\beta) = (\sin\beta, \cos\beta)$. In the limit of large m_A, m_h^2 reaches an upper limit of $2\lambda v^2$ (which tends to $\lambda_2 v^2$ for large $\tan\beta$). At tree level, $\lambda = (g^2/8)\cos^2 2\beta$, and the individual λ_j are:

$$\lambda_{1,2} \;=\; -\lambda_{345} \;=\; \frac{g^2}{4} \qquad\qquad \lambda_{5,6,7} \;=\; 0 \tag{A-7}$$

The general formula for fine-tuning Δ_p wrt a parameter p in a two-higgs doublet model that we are using can be found in the Appendix of [17]. For large $\tan\beta = v_2/v_1$ this reduces to

$$\begin{aligned}
\Delta_p &= \frac{\partial \ln v^2}{\partial \ln p} \\
&= \frac{[4\lambda_7\,(m_3^2)' - 4\lambda_7'\,m_3^2] + [\lambda_2'\,v^2 + 2(m_2^2)']\,[\lambda_{3452} + 2(m_1^2 - m_2^2)/v^2]}{2\lambda_7^2\,v^2 - \lambda_2\,[\lambda_{3452}\;v^2 + 2\,(m_1^2 - m_2^2)]} + \mathcal{O}(\cot\beta) \qquad \text{(A-8)} \\
&\to\; -\frac{1}{\lambda_2\,v^2}\left[2\,(m_2^2)' + \lambda_2'\,v^2 + 4\,v^2\left(\frac{\lambda_7\,(m_3^2)' - \lambda_7'\,m_3^2}{\lambda_{3452}\;v^2 + 2\,(m_1^2 - m_2^2)}\right)\right], \;\; (\text{if } \lambda_7| \ll |\lambda_2|, |\lambda_{3452}|)
\end{aligned}$$

where $x' = \partial x/\partial \ln p$ is the partial derivative of x wrt p.

A.2 The scalar potential: 1 Loop Leading Log (1LLL) Terms

Here we show how to obtain the one-loop corrected potential, which is "improved" to the two-loop leading log (2LLL) result in the next section. Start with

$$V^{(0)} \;=\; \bar{m}_1^2\,|H_1|^2 + \bar{m}_2^2\,|H_2|^2 - \bar{m}_3^2\,(H_1 H_2 + \text{h.c.}) + \frac{g^2}{8}\left(|H_1|^2 - |H_2|^2\right)^2 \tag{A-9}$$

This receives (field dependent threshold) corrections, computed using the Coleman-Weinberg potential [43]:

$$V^{(1)} \;=\; \frac{1}{64\pi^2}\sum_k (-1)^{2J_k}\,(2J_k+1)\,g_k\,m_k^4\left(\log\frac{m_k^2}{Q^2} - \frac{3}{2}\right) \tag{A-10}$$

where m_k is the field dependent mass, the degeneracy factor g_k is 6 for squarks, and J_k is the particle spin. All parameters in eq.(A-10) are evaluated at the scale Q using the RGEs which ignore the particle masses. The field dependent squark masses are (neglecting $O\big(g^4\big)$ terms):

$$m^2_{\tilde{t}_{1,2}} \approx M_S^2 + h_t^2 |H_2|^2 + \frac{g^2}{8}\left(|H_1|^2 - |H_2|^2\right) \mp h_t |A_t H_2 - \mu H_1^*| \quad \text{(A-11)}$$

$$m^2_{\tilde{b}_{1,2}} \approx M_S^2 + h_b^2 |H_1|^2 + \frac{g^2}{8}\left(|H_2|^2 - |H_1|^2\right) \mp h_b |A_b H_1 - \mu H_2^*| \quad \text{(A-12)}$$

and where $m_{Q,U,D}(M_S) = M_S$ is assumed. Here, M_S is the soft SUSY breaking squark mass evaluated at the squark mass scale.

One can expand the non-linear field dependence (log) in $V^{(1)}$ in inverse powers of $1/M_S$ to find the dominant threshold corrections, which come from the third generation squarks:

$$\begin{aligned} V^{(1)}_{\tilde{t}_{1,2}} \approx \frac{3}{16\pi^2}\Bigg[& t\left(h_t^4 |H_2|^4 + 2h_t^2 M_S^2 |H_2|^2 + h_t^2 |A_t H_2 - \mu H_1^*|^2\right) \\ & + h_t^4 \frac{|A_t H_2 - \mu H_1^*|^2}{M_S^2}\left(|H_2|^2 - \frac{|A_t H_2 - \mu H_1^*|^2}{12 M_S^2}\right) \\ & + \frac{g^2}{8}\left(|H_1|^2 - |H_2|^2\right)\left(2t\, h_t^2 |H_2|^2 + 2M_S^2 (t-1) + \frac{|A_t H_2 - \mu H_1^*|^2}{M_S^2}\right)\Bigg] \end{aligned} \quad \text{(A-13)}$$

$$\begin{aligned} V^{(1)}_{\tilde{b}_{1,2}} \approx \frac{3}{16\pi^2}\Bigg[& t\left(h_b^4 |H_1|^4 + 2h_b^2 M_S^2 |H_1|^2 + h_b^2 |A_b H_1 - \mu H_2^*|^2\right) \\ & + h_b^4 \frac{|A_b H_1 - \mu H_2^*|^2}{M_S^2}\left(|H_1|^2 - \frac{|A_b H_1 - \mu H_2^*|^2}{12 M_S^2}\right) \\ & + \frac{g^2}{8}\left(|H_2|^2 - |H_1|^2\right)\left(2t\, h_b^2 |H_1|^2 + 2M_S^2 (t-1) + \frac{|A_b H_1 - \mu H_2^*|^2}{M_S^2}\right)\Bigg] \end{aligned} \quad \text{(A-14)}$$

where

$$t = \log(M_S^2/Q^2) \quad \text{(A-15)}$$

When running below the EWSB scale, the inclusion of higher dimensional terms (threshold corrections) lead to a re-summation such that M_S is replaced by a mass scale related to the physical particle masses [44]. For the results of this paper, the geometric mean of the stop masses is used in the place of M_S.

The above equations are valid down to the top mass scale; below this scale threshold corrections from the top quark should also be included. The dominant effect of running below the top scale can be absorbed by setting Q in the above equations as the "running" top mass evaluated at the scale Q instead of the pole mass.

From eqs.(A-9) to (A-14) one obtains the parameters entering in the scalar potential (1), evaluated at the scale Q (below M_S), in the one-loop leading log approximation (1LLL):

$$m_1^2 = \bar{m}_1^2 - \frac{6h_b^2}{16\pi^2} M_S^2 + \frac{3}{16\pi^2}\left(2h_b^2 M_S^2 + h_b^2 A_b^2 + h_t^2\mu^2\right) t \quad \text{(A-16)}$$

$$m_2^2 = \bar{m}_2^2 - \frac{6h_t^2}{16\pi^2} M_S^2 + \frac{3}{16\pi^2}\left(2h_t^2 M_S^2 + h_t^2 A_t^2 + h_b^2\mu^2\right) t \quad \text{(A-17)}$$

$$m_3^2 = \bar{m}_3^2 + \frac{3}{16\pi^2}\left(h_t^2 A_t + h_b^2 A_b\right)\mu\, t \quad \text{(A-18)}$$

$$\lambda_1 = \frac{g^2}{4}\left(1 + \frac{3\left(h_t^2\,\mu^2 - h_b^2\,A_b^2\right)}{16\pi^2\,M_S^2}\right) + \frac{3}{8\pi^2}\left(\frac{h_b^4\,X_b}{2} - \frac{h_t^4\,\mu^4}{12M_S^4}\right) + \frac{3h_b^2}{8\pi^2}\left(h_b^2 - \frac{g^2}{4}\right) t \quad \text{(A-19)}$$

$$\lambda_2 = \frac{g^2}{4}\left(1 + \frac{3\left(h_b^2\,\mu^2 - h_t^2\,A_t^2\right)}{16\pi^2\,M_S^2}\right) + \frac{3}{8\pi^2}\left(\frac{h_t^4\,X_t}{2} - \frac{h_b^4\,\mu^4}{12M_S^4}\right) + \frac{3h_t^2}{8\pi^2}\left(h_t^2 - \frac{g^2}{4}\right) t \quad \text{(A-20)}$$

$$\lambda_{34} = -\frac{g^2}{4}\left(1 + \frac{3h_t^2\left(\mu^2 - A_t^2\right)}{32\pi^2\,M_S^2} + \frac{3h_b^2\left(\mu^2 - A_b^2\right)}{32\pi^2\,M_S^2}\right) + \frac{3\left(h_t^2 + h_b^2\right)}{16\pi^2}\,\frac{g^2}{4}\,t$$
$$+ \frac{3h_t^4}{16\pi^2}\left(\frac{\mu^2}{M_S^2} - \frac{\mu^2 A_t^2}{3M_S^4}\right) + \frac{3h_b^4}{16\pi^2}\left(\frac{\mu^2}{M_S^2} - \frac{\mu^2 A_b^2}{3M_S^4}\right) \quad \text{(A-21)}$$

$$\lambda_5 = -\frac{3h_t^4}{96\pi^2}\frac{\mu^2 A_t^2}{M_S^4} - \frac{3h_b^4}{96\pi^2}\frac{\mu^2 A_b^2}{M_S^4} \quad \text{(A-22)}$$

$$\lambda_6 = \frac{g^2}{4}\left(\frac{3\mu\left(h_b^2 A_b - h_t^2 A_t\right)}{32\pi^2\,M_S^2}\right) + \frac{3h_t^4}{96\pi^2}\,\frac{\mu^3 A_t}{M_S^4} + \frac{3h_b^4}{96\pi^2}\,\frac{\mu}{M_S}\left(\frac{A_b^3}{M_S^3} - \frac{6A_b}{M_S}\right) \quad \text{(A-23)}$$

$$\lambda_7 = \frac{g^2}{4}\left(\frac{3\mu\left(h_t^2 A_t - h_b^2 A_b\right)}{32\pi^2\,M_S^2}\right) + \frac{3h_b^4}{96\pi^2}\,\frac{\mu^3 A_b}{M_S^4} + \frac{3h_t^4}{96\pi^2}\,\frac{\mu}{M_S}\left(\frac{A_t^3}{M_S^3} - \frac{6A_t}{M_S}\right) \quad \text{(A-24)}$$

These analytic results agree with [25] which ignore the stop mixing corrections to the D-terms, but are included here for completeness. The following notation is used in this appendix.

$$X_{t,b} = \frac{2A_{t,b}^2}{M_S^2}\left(1 - \frac{A_{t,b}^2}{12M_S^2}\right) \quad \text{(A-25)}$$

A.3 The scalar potential: 2 Loop Leading Log (2LLL) Terms

The two-loop leading log (2LLL) Coleman-Weinberg potential can be found in the arXiv version of [45] to $O\big(g_3^2\,h_t^4, g_3^2\,h_b^4\big)$ and $O\big(h_t^6, h_t^4\,h_b^2, h_t^2\,h_b^4, h_b^6\big)$, see also [46, 47] for the general case. The method of the previous section may be used to determine the 2LLL contributions to the Higgs scalar potential, however here we proceed instead with an approach similar to that in [44], to RG-improve the 1-loop result into a 2LLL result. A step approximation is applied to the β-functions so that the MSSM RG eqs are used between the GUT and stop mass scale, then the 2HDM SM RG eqs between the stop and top mass scales, and finally the top is integrated out to reach the electroweak scale.

When setting the renormalisation scale in eqs (A-16) to (A-24) as $Q = M_S$, the logarithmic terms are removed but the finite corrections from stop mixing remain. These results are then used as boundary conditions for the parameters at the scale M_S. A series expansion of the RG eqs is then applied:

$$\begin{aligned}
\lambda\,(Q) &\approx \lambda\,(M_S) - \beta_\lambda\,(M_S)\;t + \frac{1}{2}\,\beta'_\lambda\,(M_S)\;t^2 + O\big(t^3\big) && \text{(A-26)}\\
&= \lambda\,(M_S) - \beta_\lambda\,(Q)\;t - \frac{1}{2}\,\beta'_\lambda\,(Q)\;t^2 + O\big(t^3\big) && \text{(A-27)}
\end{aligned}$$

where $\beta_p = \partial p/\partial \log Q^2$. Eventually, all parameters will be expressed at a scale Q as in the Coleman-Weinberg potential approach. For a β_λ-function of the form $b\,\lambda + c$, eq (A-27) becomes

$$\lambda \approx \lambda\,(M_S) - t\,[b\,\lambda\,(M_S) + c] + t^2\left[b\,c - \frac{1}{2}\,\beta'_\lambda + O(\lambda)\right] \qquad \text{(A-28)}$$

where the couplings are evaluated at the scale Q unless stated otherwise. The β-functions for the 2HDM SM [48] are listed below, neglecting $O\big(h_\tau^2\big)$ terms, and with the β_{λ_i}-functions also neglecting $O\big(g^4, g^2\lambda_i, \lambda_i^2\big)$ terms:

$$\begin{aligned}
16\pi^2\,\beta_{m_1^2} &= 3h_b^2\,m_1^2 + O\left(g^2 m^2\right)\\
16\pi^2\,\beta_{m_2^2} &= 3h_t^2 m_2^2 + O\left(g^2 m^2\right)\\
16\pi^2\,\beta_{m_3^2} &= \frac{3}{2}\left(h_t^2 + h_b^2\right) m_3^2 + O\left(g^2 m^2\right) && \text{(A-29)}
\end{aligned}$$

$$
\begin{aligned}
16\pi^2\,\beta_{\lambda_1} &\approx 6h_b^2\left(\lambda_1 - h_b^2\right)\\
16\pi^2\,\beta_{\lambda_2} &\approx 6h_t^2\left(\lambda_2 - h_t^2\right)\\
16\pi^2\,\beta_{\lambda_3} &\approx 3\lambda_3\left(h_t^2 + h_b^2\right) - 6h_t^2h_b^2\\
16\pi^2\,\beta_{\lambda_4} &\approx 3\lambda_4\left(h_t^2 + h_b^2\right) + 6h_t^2h_b^2\\
16\pi^2\,\beta_{\lambda_5} &\approx 3\lambda_5\left(h_t^2 + h_b^2\right)\\
16\pi^2\,\beta_{\lambda_6} &\approx \lambda_6\left(\frac{9}{2}\,h_b^2 + \frac{3}{2}\,h_t^2\right)\\
16\pi^2\,\beta_{\lambda_7} &\approx \lambda_7\left(\frac{9}{2}\,h_t^2 + \frac{3}{2}\,h_b^2\right) \qquad \text{(A-30)}
\end{aligned}
$$

and finally

$$
16\pi^2\,\beta_{h_t^2} \approx h_t^2\left(\frac{9}{2}\,h_t^2 + \frac{1}{2}\,h_b^2 - 8g_3^2 - \frac{9}{4}\,g_2^2 - \frac{17}{12}\,g_1^2\right) \qquad \text{(A-31)}
$$

$$
16\pi^2\,\beta_{h_b^2} \approx h_b^2\left(\frac{9}{2}\,h_b^2 + \frac{1}{2}\,h_t^2 + h_\tau^2 - 8g_3^2 - \frac{9}{4}\,g_2^2 - \frac{5}{12}\,g_1^2\right) \qquad \text{(A-32)}
$$

Using (A-28), the analytic 2-loop results in [25] are then recovered when the same level of approximation is considered. For example,

$$
\lambda_2 \approx \left[\lambda_2\left(M_S\right) - \lambda_2\,a_2\,t\right] - b_2\,t + \left[a_2\,b_2 + \frac{3h_t^2}{16\pi^2}\left(2\beta_{h_t^2} - \beta_{\lambda_2}\right) + O(\lambda)\right]t^2 \qquad \text{(A-33)}
$$

$$
= \left[\lambda_2\left(M_S\right) - \lambda_2\,\frac{6h_t^2}{16\pi^2}\,t\right] + \frac{3h_t^4}{8\pi^2}\left[t + \frac{1}{16\pi^2}\left(\frac{3}{2}\,h_t^2 + \frac{1}{2}\,h_b^2 - 8g_3^2\right)t^2\right] \qquad \text{(A-34)}
$$

The couplings entering in the expression of $\lambda_2\left(M_S\right)$ are re-expressed in terms of their values at the scale Q, (with a logarithmic correction which compensates for the running below M_S):

$$
h_t^4(M_S) = h_t^4\left(1 + \frac{t}{16\pi^2}\left(9h_t^2 + h_b^2 - 16g_3^2\right) + O\left(g^2\,t, t^2\right)\right) \qquad \text{(A-35)}
$$

$$
h_b^4(M_S) = h_b^4\left(1 + \frac{t}{16\pi^2}\left(9h_b^2 + h_t^2 - 16g_3^2\right) + O\left(g^2\,t, t^2\right)\right) \qquad \text{(A-36)}
$$

This leads to the following expression, in agreement with [25], when the stop mixing contributions to the D-terms in the potential are neglected:

$$
\begin{aligned}
\lambda_2 \approx{}& \frac{g^2}{4}\left(1 - \frac{3h_t^2}{8\pi^2}\,t\right) - \frac{3h_b^4}{96\pi^2}\,\frac{\mu^4}{M_S^4}\left[1 + \frac{t}{16\pi^2}\left(9h_b^2 - 5h_t^2 - 16g_3^2\right)\right]\\
&+ \frac{3h_t^4}{8\pi^2}\left[t + \frac{X_t}{2} + \frac{t}{16\pi^2}\left(\frac{3h_t^2}{2} + \frac{h_b^2}{2} - 8g_3^2\right)\left(X_t + t\right)\right] \qquad \text{(A-37)}
\end{aligned}
$$

Note that these results assume that the CP odd Higgs mass is not decoupled. If this is the case, the usual SM β-functions should be used. The effective quartic coupling at the EW scale when $m_A \lesssim M_S$ is given by:

$$\begin{aligned}\lambda &\approx \frac{g^2}{8}\cos^2 2\beta\Big[1-\frac{3}{16\pi^2}\left(h_b^2+h_t^2+\left(h_b^2-h_t^2\right)\sec 2\beta\right)t\Big] \\ &+\frac{3\,h_t^4}{16\pi^2}\sin^4\beta\left[t+\frac{\tilde{X}_t}{2}+\frac{1}{16\pi^2}\left(\frac{3\,h_t^2}{2}+\frac{h_b^2}{2}-8g_3^2\right)\left(\tilde{X}_t\,t+t^2\right)+\delta_1\right] \\ &+\frac{3\,h_b^4}{16\pi^2}\cos^4\beta\left[t+\frac{\tilde{X}_b}{2}+\frac{1}{16\pi^2}\left(\frac{3\,h_b^2}{2}+\frac{h_t^2}{2}-8g_3^2\right)\left(\tilde{X}_b\,t+t^2\right)+\delta_2\right] \qquad \text{(A-38)}\end{aligned}$$

with the following notation:

$$\delta_1 = \frac{3t\left(h_b^2-h_t^2\right)}{16\pi^2}\,\frac{\tilde{A}_t\,\mu\cot\beta}{M_S^2}\left(1-\frac{\tilde{A}_t^2}{6M_S^2}\right) \qquad \text{(A-39)}$$

$$\delta_2 = \frac{3t\left(h_t^2-h_b^2\right)}{16\pi^2}\,\frac{\tilde{A}_b\,\mu\tan\beta}{M_S^2}\left(1-\frac{\tilde{A}_b^2}{6M_S^2}\right) \qquad \text{(A-40)}$$

where $\tilde{X}_{t,b}$ is defined as $X_{t,b}(A_{t,b}\to\tilde{A}_{t,b})$ with

$$\begin{aligned}\tilde{A}_t &= A_t-\mu\cot\beta \\ \tilde{A}_b &= A_b-\mu\tan\beta \qquad \text{(A-41)}\end{aligned}$$

A similar but distinct result is obtained when $m_A \sim M_S$ (notably no δ_i terms and a different dependence on $\tan\beta$ and the mixed Yukawa couplings). The threshold corrections are dependent on where the CP odd Higgs decouples. The same procedure has been applied to determine the 2LLL threshold corrections to the mass terms.

References

[1] J. R. Ellis, K. Enqvist, D. V. Nanopoulos and F. Zwirner, "Observables In Low-Energy Superstring Models," Mod. Phys. Lett. A **1** (1986) 57.

[2] R. Barbieri and G. F. Giudice, "Upper Bounds On Supersymmetric Particle Masses," Nucl. Phys. B **306** (1988) 63;

[3] R. Barbieri and A. Strumia, "About the fine-tuning price of LEP," Phys. Lett. B **433** (1998) 63 [arXiv:hep-ph/9801353].

[4] P. H. Chankowski, J. R. Ellis and S. Pokorski, "The fine-tuning price of LEP," Phys. Lett. B **423** (1998) 327 [arXiv:hep-ph/9712234].

[5] P. H. Chankowski, J. R. Ellis, M. Olechowski and S. Pokorski, "Haggling over the fine-tuning price of LEP," Nucl. Phys. B **544** (1999) 39 [arXiv:hep-ph/9808275].

[6] G. L. Kane and S. F. King, "Naturalness implications of LEP results," Phys. Lett. B **451** (1999) 113 [arXiv:hep-ph/9810374].

[7] G. F. Giudice and R. Rattazzi, "Living dangerously with low-energy supersymmetry," Nucl. Phys. B **757** (2006) 19 [arXiv:hep-ph/0606105].

[8] A. Romanino and A. Strumia, "Are heavy scalars natural in minimal supergravity?," Phys. Lett. B **487** (2000) 165 [arXiv:hep-ph/9912301].

[9] D. Horton and G. G. Ross, "Naturalness and Focus Points with Non-Universal Gaugino Masses," arXiv:0908.0857 [hep-ph].

[10] R. Dermisek and J. F. Gunion, "The NMSSM Solution to the Fine-Tuning Problem, Precision Electroweak Constraints and the Largest LEP Higgs Event Excess," Phys. Rev. D **76** (2007) 095006 [arXiv:0705.4387 [hep-ph]].

[11] J. A. Casas, J. R. Espinosa and I. Hidalgo, "The MSSM fine tuning problem: A way out," JHEP **0401** (2004) 008 [arXiv:hep-ph/0310137]; "A relief to the supersymmetric fine tuning problem," [arXiv:hep-ph/0402017].

[12] R. Barbieri and A. Strumia, "What is the limit on the Higgs mass?," Phys. Lett. B **462** (1999) 144 [arXiv:hep-ph/9905281].

[13] J. L. Feng and K. T. Matchev, "Focus Point Supersymmetry: Proton Decay, Flavor and CP Violation, and the Higgs Boson Mass," Phys. Rev. D **63** (2001) 095003 [arXiv:hep-ph/0011356]; J. L. Feng, K. T. Matchev and T. Moroi, "Multi-TeV scalars are natural in minimal supergravity," Phys. Rev. Lett. **84** (2000) 2322 [arXiv:hep-ph/9908309]; J. L. Feng, K. T. Matchev and F. Wilczek, "Neutralino Dark Matter in Focus Point Supersymmetry," Phys. Lett. B **482** (2000) 388 [arXiv:hep-ph/0004043].

[14] K. L. Chan, U. Chattopadhyay and P. Nath, "Naturalness, weak scale supersymmetry and the prospect for the observation of supersymmetry at the Tevatron and at the LHC," Phys. Rev. D **58** (1998) 096004 [arXiv:hep-ph/9710473].

[15] P. H. Chankowski, J. R. Ellis, K. A. Olive and S. Pokorski, "Cosmological fine tuning, supersymmetry, and the gauge hierarchy problem," Phys. Lett. B **452** (1999) 28 [arXiv:hep-ph/9811284].

[16] J. R. Ellis, S. F. King and J. P. Roberts, "The Fine-Tuning Price of Neutralino Dark Matter in Models with Non-Universal Higgs Masses," JHEP **0804** (2008) 099 [arXiv:0711.2741 [hep-ph]].

[17] S. Cassel, D. M. Ghilencea and G. G. Ross, "Fine tuning as an indication of physics beyond the MSSM," Nucl. Phys. B **825** (2010) 203 [arXiv:0903.1115 [hep-ph]].

[18] S. Cassel, D. M. Ghilencea and G. G. Ross, "Testing SUSY," arXiv:0911.1134 [hep-ph], submitted to Physics Letters B.

[19] R. Barate *et al.* [LEP Working Group for Higgs boson searches], "Search for the standard model Higgs boson at LEP," Phys. Lett. B **565**, 61 (2003) [arXiv:hep-ex/0306033]; S. Schael *et al.* [ALEPH Collaboration], "Search for neutral MSSM Higgs bosons at LEP," Eur. Phys. J. C **47**, 547 (2006) [arXiv:hep-ex/0602042].

[20] M. Dine, N. Seiberg and S. Thomas, "Higgs Physics as a Window Beyond the MSSM (BMSSM)," Phys. Rev. D **76** (2007) 095004 [arXiv:0707.0005 [hep-ph]].

[21] I. Antoniadis, E. Dudas, D. M. Ghilencea and P. Tziveloglou, "MSSM with Dimension-five Operators (MSSM_5)," Nucl. Phys. B **808** (2009) 155 [arXiv:0806.3778 [hep-ph]].

[22] I. Antoniadis, E. Dudas, D. M. Ghilencea and P. Tziveloglou, "MSSM Higgs with dimension-six operators," arXiv:0910.1100 [hep-ph].

[23] M. Carena, K. Kong, E. Ponton and J. Zurita, "Supersymmetric Higgs Bosons and Beyond," arXiv:0909.5434 [hep-ph].

[24] S. P. Martin and M. T. Vaughn, "Two Loop Renormalization Group Equations For Soft Supersymmetry Breaking Couplings," Phys. Rev. D **50**, 2282 (1994) [Erratum-ibid. D **78**, 039903 (2008)] [arXiv:hep-ph/9311340].

[25] M. S. Carena, J. R. Espinosa, M. Quiros and C. E. M. Wagner, "Analytical expressions for radiatively corrected Higgs masses and couplings in the MSSM," Phys. Lett. B **355** (1995) 209 [arXiv:hep-ph/9504316].

[26] P. Ciafaloni and A. Strumia, "Naturalness upper bounds on gauge mediated soft terms," Nucl. Phys. B **494** (1997) 41 [arXiv:hep-ph/9611204]; L. Giusti, A. Romanino and A. Strumia, "Natural ranges of supersymmetric signals," Nucl. Phys. B **550** (1999) 3 [arXiv:hep-ph/9811386].

[27] N. Chen, D. Feldman, Z. Liu and P. Nath, "SUSY and Higgs Signatures Implied by Cancellations in $b \to s\gamma$," arXiv:0911.0217 [hep-ph].

[28] S. Dimopoulos and G. F. Giudice, "Naturalness constraints in supersymmetric theories with nonuniversal soft terms," Phys. Lett. B **357** (1995) 573 [arXiv:hep-ph/9507282].

[29] B. C. Allanach, "SOFTSUSY: A C++ program for calculating supersymmetric spectra," Comput. Phys. Commun. **143** (2002) 305 [arXiv:hep-ph/0104145].

[30] A. Djouadi, J. L. Kneur and G. Moultaka, "SuSpect: A Fortran code for the supersymmetric and Higgs particle spectrum in the MSSM," Comput. Phys. Commun. **176**, 426 (2007) [arXiv:hep-ph/0211331].

[31] B. C. Allanach, A. Djouadi, J. L. Kneur, W. Porod and P. Slavich, "Precise determination of the neutral Higgs boson masses in the MSSM," JHEP **0409** (2004) 044 [arXiv:hep-ph/0406166].

[32] T. Hahn, S. Heinemeyer, W. Hollik, H. Rzehak and G. Weiglein, "FeynHiggs: A program for the calculation of MSSM Higgs-boson observables - Version 2.6.5," Comput. Phys. Commun. **180**, 1426 (2009).

[33] G. Hinshaw *et al.* [WMAP Collaboration], "Five-Year Wilkinson Microwave Anisotropy Probe (WMAP) Observations:Data Processing, Sky Maps, & Basic Results," Astrophys. J. Suppl. **180** (2009) 225 [arXiv:0803.0732 [astro-ph]].

[34] The Tevatron Electroweak Working Group (TevEWWG) and CDF Collaboration and D0 Collab, "A Combination of CDF and D0 Results on the Mass of the Top Quark," [arXiv:0803.1683 [hep-ex]].

[35] G. Belanger, F. Boudjema, A. Pukhov and A. Semenov, "micrOMEGAs2.0: A program to calculate the relic density of dark matter in a generic model," Comput. Phys. Commun. **176**, 367 (2007) [arXiv:hep-ph/0607059].

[36] B.C. Allanach et al, "The Snowmass points and Slopes: Benchmarks for SUSY Searches", Eur.Phys.J.C25:113-123,2002 [arXiv: hep-ph/0202233].

[37] H. Baer, V. Barger, A. Lessa and X. Tata, "Supersymmetry discovery potential of the LHC at $\sqrt{s}$ =10 and 14 TeV without and with missing E_T," JHEP **0909** (2009) 063 [arXiv:0907.1922 [hep-ph]].

[38] R. Barbieri, F. Caravaglios, M. Frigeni and M. L. Mangano, "Production and leptonic decays of charginos and neutralinos in hadronic collisions," Nucl. Phys. B **367** (1991) 28

[39] H. Baer, A. Belyaev, T. Krupovnickas and J. O'Farrill, "Indirect, direct and collider detection of neutralino dark matter," JCAP **0408** (2004) 005 [arXiv:hep-ph/0405210].

[40] W. Vandelli, "Prospects for the detection of chargino - neutralino direct production with the ATLAS detector at the LHC," CERN-THESIS-2007-072.

[41] See also the CMS study: W. de Boer, I. Gebauer, M. Niegel, C. Sander, M. Weber, V. Zhukov and K. Mazumdar, "Trilepton final state from neutralino chargino production in mSUGRA," CERN-CMS-NOTE-2006-113.

[42] S. Davidson and H. E. Haber, "Basis-independent methods for the two-Higgs-doublet model," Phys. Rev. D **72** (2005) 035004 [Erratum-ibid. D **72** (2005) 099902] [arXiv:hep-ph/0504050].

[43] S. R. Coleman and E. J. Weinberg, "Radiative Corrections As The Origin Of Spontaneous Symmetry Breaking," Phys. Rev. D **7** (1973) 1888.

[44] M. S. Carena, M. Quiros and C. E. M. Wagner, "Effective potential methods and the Higgs mass spectrum in the MSSM," Nucl. Phys. B **461** (1996) 407 [arXiv:hep-ph/9508343].

[45] J. R. Espinosa and R. J. Zhang, "Complete two-loop dominant corrections to the mass of the lightest CP-even Higgs boson in the minimal supersymmetric standard model," Nucl. Phys. B **586** (2000) 3 [arXiv:hep-ph/0003246].

[46] S. P. Martin, "Two-loop effective potential for a general renormalizable theory and softly broken supersymmetry," Phys. Rev. D **65** (2002) 116003 [arXiv:hep-ph/0111209].

[47] S. P. Martin, "Two-loop effective potential for the minimal supersymmetric standard model," Phys. Rev. D **66** (2002) 096001 [arXiv:hep-ph/0206136].

[48] H. E. Haber and R. Hempfling, "The Renormalization group improved Higgs sector of the minimal supersymmetric model," Phys. Rev. D **48**, 4280 (1993) [arXiv:hep-ph/9307201].

[49] R. Hempfling and A. H. Hoang, "Two loop radiative corrections to the upper limit of the lightest Higgs boson mass in the minimal supersymmetric model," Phys. Lett. B **331** (1994) 99 [arXiv:hep-ph/9401219].